Electronic Supplementary Material (ESI) for Physical Chemistry Chemical Physics.
This journal is © the Owner Societies 2017

Aqueous dispersions of nanostructures formed through the self-assembly of iminolipids with exchangeable hydrophobic termini

Wen Li,[1,2] Daryl McManus,[1] Han Liu,[3] Cinzia Casiraghi[1] and Simon J. Webb[1,2,*]

1. School of Chemistry, University of Manchester, Oxford Road, Manchester M13 9PL, United Kingdom

2. Manchester Institute of Biotechnology, University of Manchester, 131 Princess St, Manchester M1 7DN, United Kingdom

3. Materials Science Centre, School of Materials, the University of Manchester, Manchester M13 9PL, United Kingdom

Table of Contents

1. Instruments

All ^{1}H and ^{13}C nuclear magnetic resonance (NMR) spectra were obtained using a Bruker DPX spectrometer (at 400 MHz), with an internal deuterium lock. Chemical shifts are quoted in parts per million (ppm) and coupling constants (*J*) are quoted in Hz to the nearest 0.5 Hz. ^{1}H NMR were referenced to the residual deuterated solvent peak ($CDCl_3$ 7.26; D_2O 4.79 ppm) and ^{13}C NMR were referenced to the carbon resonance of the solvent ($CDCl_3$ 77.0 ppm). Multiplicities are denoted as s (singlet), d (doublet), t (triplet), q (quartet), m (multiplet), br. (broad), or some combination of these where appropriate. Where ^{1}H NMR spectra were run in D_2O exchangeable protons (NH, OH) are reported only when observed. Assignments were made with the aid of 2D ^{1}H-COSY and HMQC experiments.

Fourier transform Infrared (FTIR) spectra were recorded on a Bruker Alpha-p instrument using OPUS 6.5 software package, data processed analysed using Spekwin32 software package. Only absorption maxima of interest are reported and quoted in wavenumbers (cm^{-1}). Low and high resolution mass spectra were recorded by staff at the University of Manchester. Electrospray (ES) spectra were recorded on a Waters Platform II. High resolution mass spectra (HRMS) were recorded on a Thermo Finnigan MAT95XPand are accurate to ±0.001 Da. All pH measurements recorded on a HANNA pH 212-microprocessor pH meter.

Samples assessed by Dynamic Light Scattering (DLS) were measured in HPLC grade water at 25 °C on a Malvern Zetasizer Nano S (He-Ne laser 633 nm) instrument. Fluorescence spectroscopy measurements were carried on a Perkin-Elmer LS55 fluorimeter with Julabo F25-HE water circulator for temperature control at 25 °C. Liquid Chromatography - Mass Spectrometry (LC-MS) was performed on a LC-MSD-Trap-SL instrument using an Agilent XDB C18 4.6 × 150 mm column using a H_2O/acetonitrile acidified with 0.1 % TFA (vol/vol). The injection volume was 10 µL and the flow rate was 0.5 mL/min. Sonication was performed using a TranssonicTM T460 bath-type sonicator. UV-Visible measurements (200-700 nm) were collected using “Sigma” brand silica (quartz) cuvettes with 10 mm path lengths. Data were recorded on an Agilent Technologies Cary 60 UV-Visible spectrometer (600 nm/min) with three cycle counts (0.1 min/cycle). Scanning Electron Microscope (SEM) was performed with FEI Quanta 650 FEG-(E) SEM instrument. Transmission Electron Microscopy (TEM) was performed using a Phillips CM20 200 kV instrument, equipped with CCD camera.

Aqueous graphene dispersions were produced using a Hilsonic 600 W bath sonicator kept at constant temperature. Centrifugation was performed using a Sigma 1-14k centrifuge. UV-Visible

measurements (200-800 nm) of graphene dispersions were collected using a Cary 5000 spectrometer. Atomic force microscopy (**AFM**) was performed using a Bruker Multimode 8 in peak force tapping mode.

1. Materials and general experimental procedures

2.1 Materials

All reactions were carried out under an atmosphere of nitrogen using standard anhydrous techniques. All synthetic reagents were either obtained from commercially available sources (Sigma Aldrich and Fisher Scientific) and were used without further purification or were prepared following published procedures (where indicated). Reactions performed at 0 °C were done so using an ice bath. All products were dried on a rotary evaporator followed by connection to a high vacuum system to remove any residual solvent. Flash chromatography was performed on silica gel (Merck 60H, 40-60 nm, 230 – 300 mesh). Analytical thin layer chromatography (TLC) was performed on Merck silica gel 60 F_{245} plates and were visualised by UV (254 nm) and phosphomolybdic acid dips where appropriate.

Graphite (99.5 % grade, purchased from Graphexel) and h-BN (98 % grade, Sigma Aldrich) were used for liquid phase exfoliation (LPE) experiments. Deionised water (10 mL, conductivity of 18.2 MΩ·cm) was obtained from a Millipore Milli-Q water purification system.

2.2 General experimental procedures

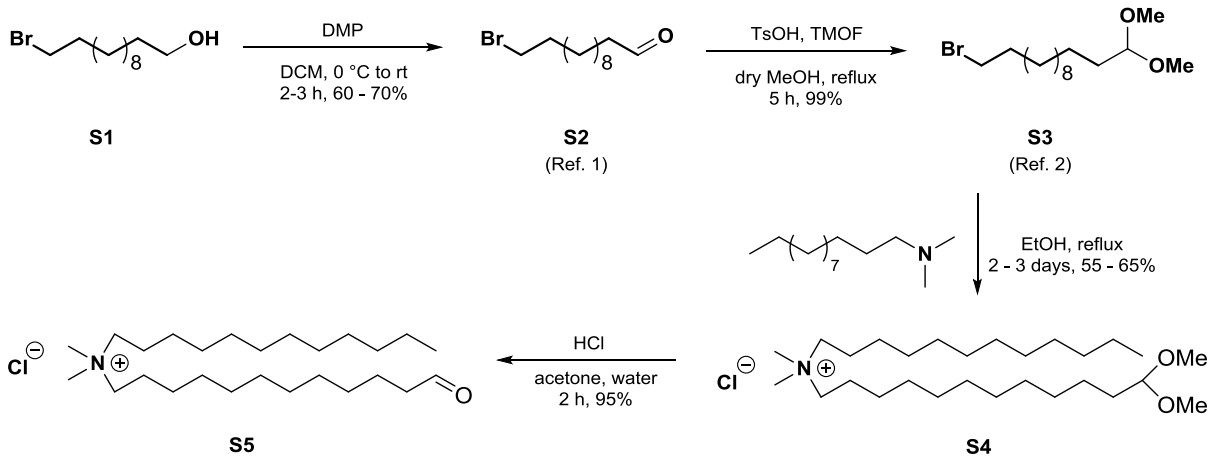

Scheme S1. Synthesis of lipid **1** (**S5**).

2.3 Abbreviations

TFA, trifluoroacetic acid; DMP, Dess-Martin periodinane; DCM, dichloromethane; TsOH, p-toluenesulfonic acid; TMOF, trimethyl orthoformate; a.u., arbitrary unit; ACN, acetonitrile; UV, ultraviolet; GPC, gel permeation chromatography; AFM, atomic force microscopy; RPM, revolutions per minute; h-BN, hexagonal boron nitride.

3. Synthetic procedures

3.1 12-Bromododecanal (S2)

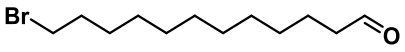

S2

12-Bromododecanol **S1** (132.6 mg, 0.5 mmol) was dissolved in dichloromethane (5 mL) and the mixture was cooled to 0 ℃ in an ice bath. Then Dess-Martin periodinane (360 mg, 0.7 mmol, 1.4 eq.) was added at 0 ℃. After stirring at room temperature (4 h), the reaction mixture was diluted with ether (5 mL) and poured into saturated $NaHCO_3$ (10 mL) and saturated $Na_2S_2O_3$ solution (10 mL). The resulting mixture was stirred for another 30 mins, extracted with DCM and combined organic layers were washed with saturated aqueous $NaHCO_3$ solution, brine and dried over $MgSO_4$. The organic solvent was removed under reduced pressure, and the residue was purified by column chromatography (petroleum ether/ethyl acetate 19:1) to give 12-bromododecanal **S2** (79 mg, 0.30 mmol, 60 %, white solid). $\boldsymbol{R_f}$ = 0.2 (petroleum ether/ethyl acetate 19:1). **^{1}H-NMR** (400 MHz, $CDCl_3$): δ_H 9.77 (1H, s, C*H*O, ^3J = 1.8 Hz), 3.41 (2H, t, Br-CH_2, ^3J = 6.8 Hz), 2.42 (2H, m, CHO-CH_2), 1.85 (2H, m, Br-CH_2-CH_2), 1.63 (2H, m, CHO-CH_2-CH_2), 1.42 (2H, m, CHO-$(CH_2)_2$-CH_2), 1.28 (14H, m, $(CH_2)_6$). ***m/z*** **(ES^+)** 262.2 ($[M + H]^+$, 100%). The spectral data matched that reported by Porter *et al*.[1]

3.2 12-Bromo-1,1-dimethoxy-dodecane (S3)

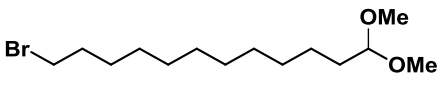

S3

12-Bromododecanal **S2** (170 mg, 0.65 mmol) was dissolved in dry methanol (5 mL) and a catalytic amount of *p*-toluenesulfonic (TsOH, 3 mg, 0.02 mmol, 0.03 eq.) and trimethyl orthoformate (TMOF, 76 mg, 0.08 mL, 0.72 mmol, 1.1 eq.) were added. The mixture was heated to reflux under a nitrogen atmosphere for 5 hours. Then the solution was cooled down, and the reaction was quenched by the

addition of saturated aqueous sodium bicarbonate solution (2 mL) and extracted with diethylether (10 mL). The organic layer was isolated and washed with water and brine, dried over $MgSO_4$, filtered and concentrated. 12-Bromo-1,1-dimethoxydodecane **S3** was collected as colourless oil (198 mg, 0.64 mmol, 99%) and was used without any further purification. **^{1}H-NMR** (400 MHz, $CDCl_3$): δ_H 4.36 (1H, t, OMe-C*H*, ^3J = 5.8 Hz), 3.41 (2H, t, Br-CH_2, ^3J = 6.8 Hz), 3.31 (6H, s, OCH_3×*2*), 1.85 (2H, m, Br-CH_2-CH_2), 1.57 (2H, m, OMe-CH_2-CH_2), 1.42-1.27 (16H, m, $(CH_2)_8$). **HRMS (ES$^+$)**: calcd for [M(79Br) + Na]$^+$, 331.1250, found 331.1229. The spectral data matched that reported by Hiromichi *et al*.[2]

3.3 (12,12-Dimethoxydodecyl)dodecyldimethyl ammonium bromide (S4)

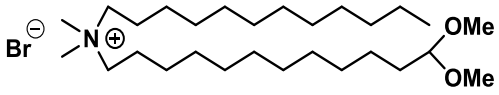

S4

A mixture of 12-bromo-1,1-dimethoxydodecane **S3** (230 mg, 0.75 mmol) and *N,N*-dimethyldodecylamine (192 mg, 0.25 mL, 0.9 mmol, 1.2 eq.) in ethanol (10 mL) was stirred at reflux for 2-3 days. The solvent was removed under reduced pressure and the resulting yellowish oil was washed with hexane (3 mL × 3) several times to remove unreacted organic residues. Compound **S4** was used without further purification (206 mg, 0.47 mmol, 62%, yellowish solid). **^{1}H-NMR** (400 MHz, $CDCl_3$): δ_H 4.35 (1H, t, OMe-C*H*-CH_2, ^3J = 5.8 Hz), 3.51 (4H, m, N-CH_2 × 2), 3.40 (6H, s, N-CH_3 × 2), 3.31 (6H, s, (O*Me*) × 2), 1.69 (4H, m, N-CH_2-CH_2 × 2), 1.59 (2H, m, MeO-CH_2-CH_2), 1.25 (36H, m, $(CH_2)_{17}$), 0.88 (3H, t, CH_3-CH_2, ^3J = 6.8 Hz); **^{13}C-NMR** (100 MHz, $CDCl_3$): δ_C 104.6, 63.8 (× 2), 52.7 (× 2), 51.4 (× 2), 43.1, 32.5, 31.9, 29.6, 29.5 (× 2), 29.5 (× 2), 29.4 (× 2), 29.4 (× 2), 29.4 (× 2), 29.3, 29.2, 26.2, 24.6, 22.8, 22.7, 14.1; **IR** (cm^{-1}): 3437, 3382, 1466 (C-OMe); ***m/z*** **(ES$^+$)** 442.6 (M^+, 31%), 428.6 $[M\text{-}CH_2]^+$, 100%) ; **HRMS (ES$^+$)**: calcd for M^+: 442.4624, found: 442.4619 (100%).

3.4 (12-Oxododecyl)dodecyldimethylammonium chloride (S5)

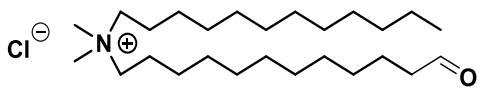

S5

Acetal **S4** (130 mg, 0.29 mmol) was dissolved in a mixture of acetone (4 mL) and distilled water (2 mL), then treated with hydrochloric acid (1M solution in water, 0.29 mL, 0.029 mmol, 0.1 eq.). The reaction mixture was stirred at room temperature for 2 h and washed with saturated sodium bicarbonate solution (3 mL) and DCM (10 mL). The combined organic layers were washed with saturated aqueous $NaHCO_3$ solution, brine and dried over $MgSO_4$. DCM was removed under reduced

pressure to give compound **S5** (109 mg, 0.28 mmol, 95 %, white solid). **^{1}H-NMR** (400 MHz, $CDCl_3$): δ_H 9.76 (1H, t, C*H*O, ^{3}J = 1.8 Hz), 3.50 (4H, m, N-C*H*$_2$ × 2), 3.40 (6H, s, N-C*H*$_3$ × 2), 2.42 (2H, td, CHO-CH-C*H*$_2$, ^{3}J = 1.8 Hz, 7.4 Hz), 1.66 (4H, m, N-CH_2-C*H*$_2$ × 2), 1.55 (2H, m, CHO-CH-CH_2-C*H*$_2$), 1.26 (32H, m, (C*H*$_2$)$_{16}$), 0.88 (3H, t, C*H*$_3$-CH_2, ^{3}J = 6.8 Hz); **^{13}C-NMR** (100 MHz, $CDCl_3$): δ_C 203.1, 63.7 (× 2), 51.6, 51.4, 43.9, 32.4, 31.9, 30.2, 29.9, 29.6, 29.4, 29.4 (× 2), 29.3 (× 2), 29.2, 29.2, 29.1, 26.9, 26.3, 23.0, 22.8, 22.7, 22.0, 14.1; **IR** (cm^{-1}): 1725 (C=O); ***m/z* (ES$^+$)** 397 (M^+, 39%); **HRMS (ES$^+$)**: calcd for M^+: 396.4205, found: 396.4200.

3.5 NMR spectra of novel compounds

^{1}H NMR Spectra

S2 ($CDCl_3$, 400 MHz)

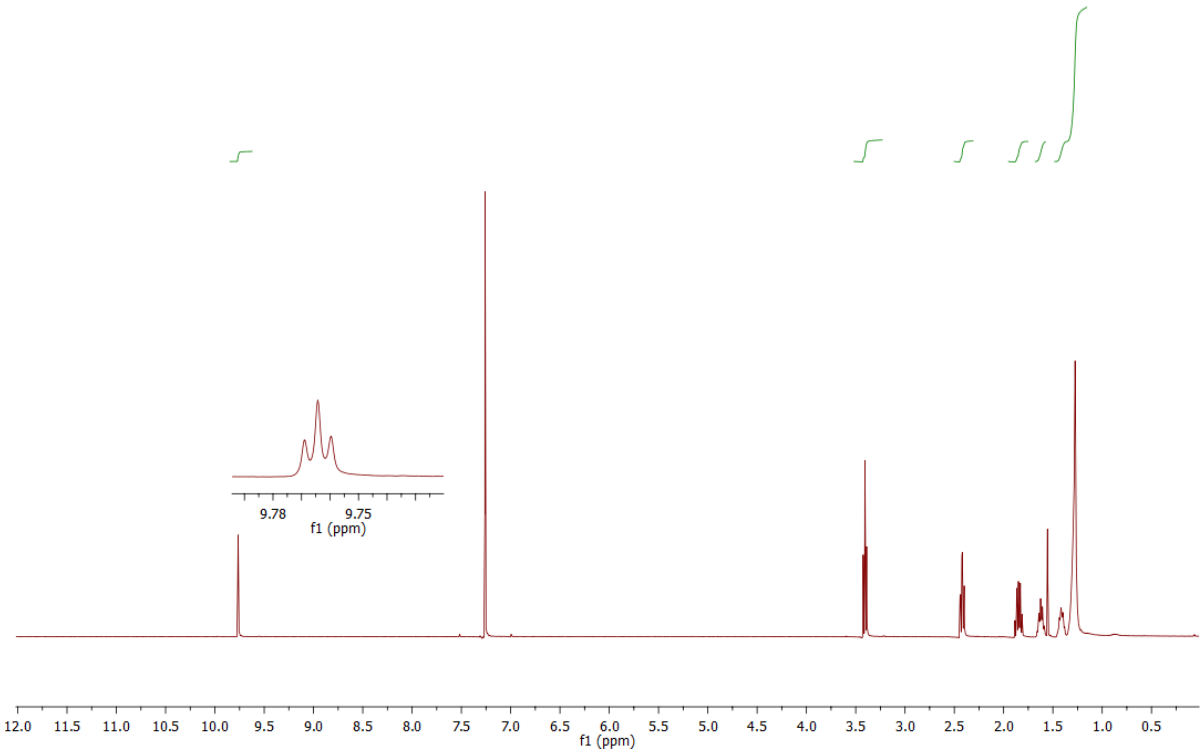

S3 ($CDCl_3$, 400 MHz)

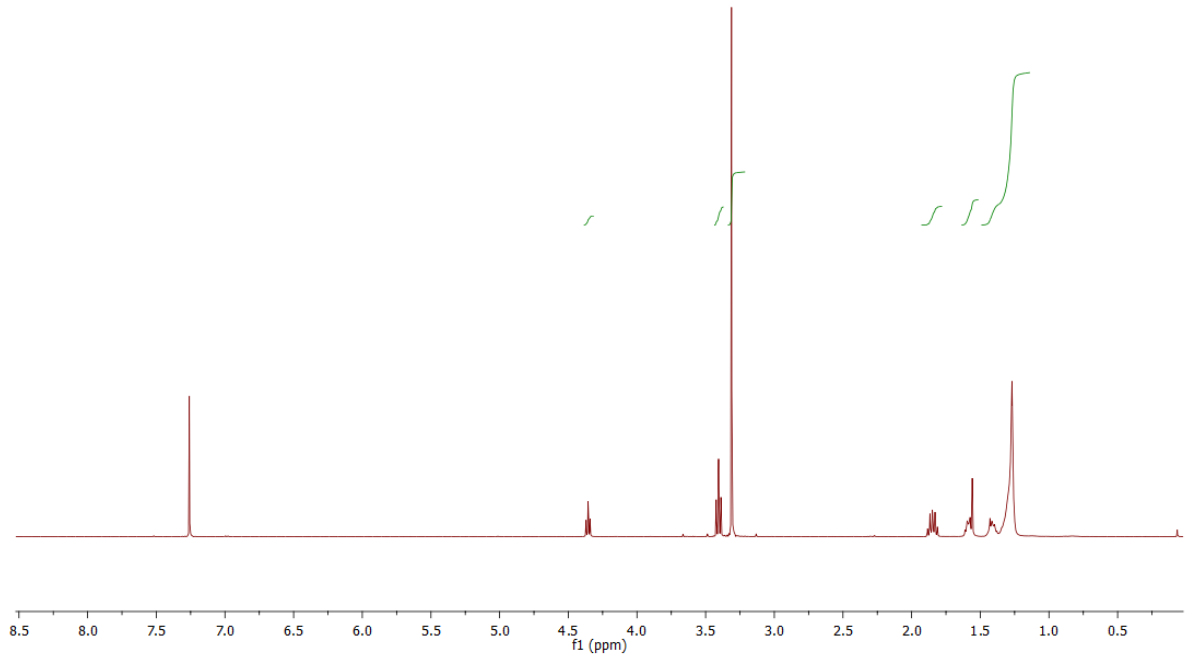

S4 ($CDCl_3$, 400 MHz)

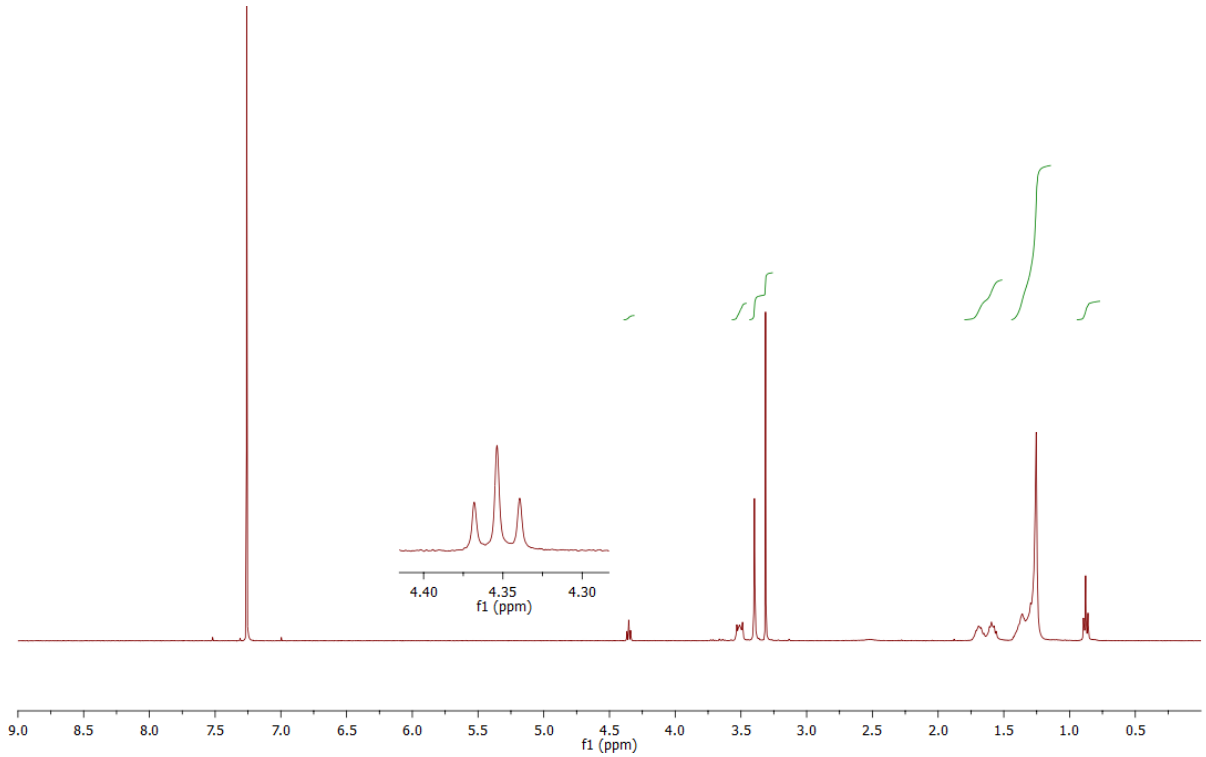

S5 ($CDCl_3$, 400 MHz)

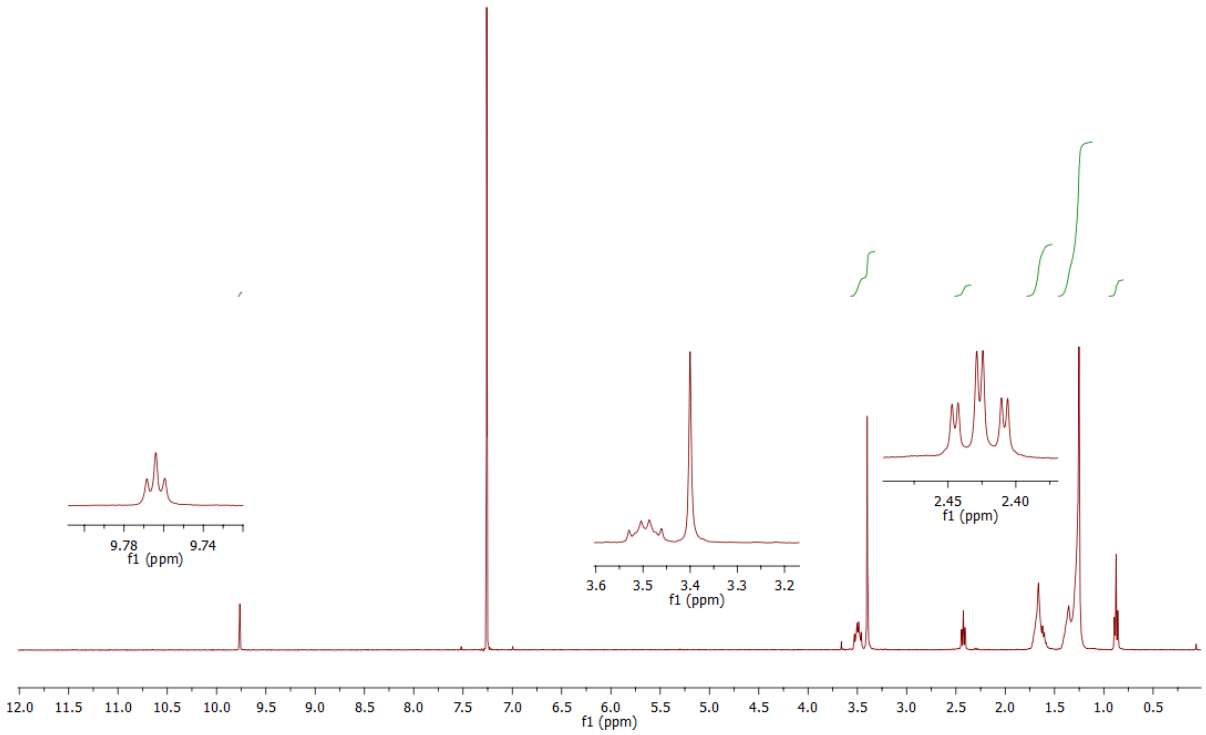

^{13}C NMR Spectra

S4 ($CDCl_3$, 100 MHz)

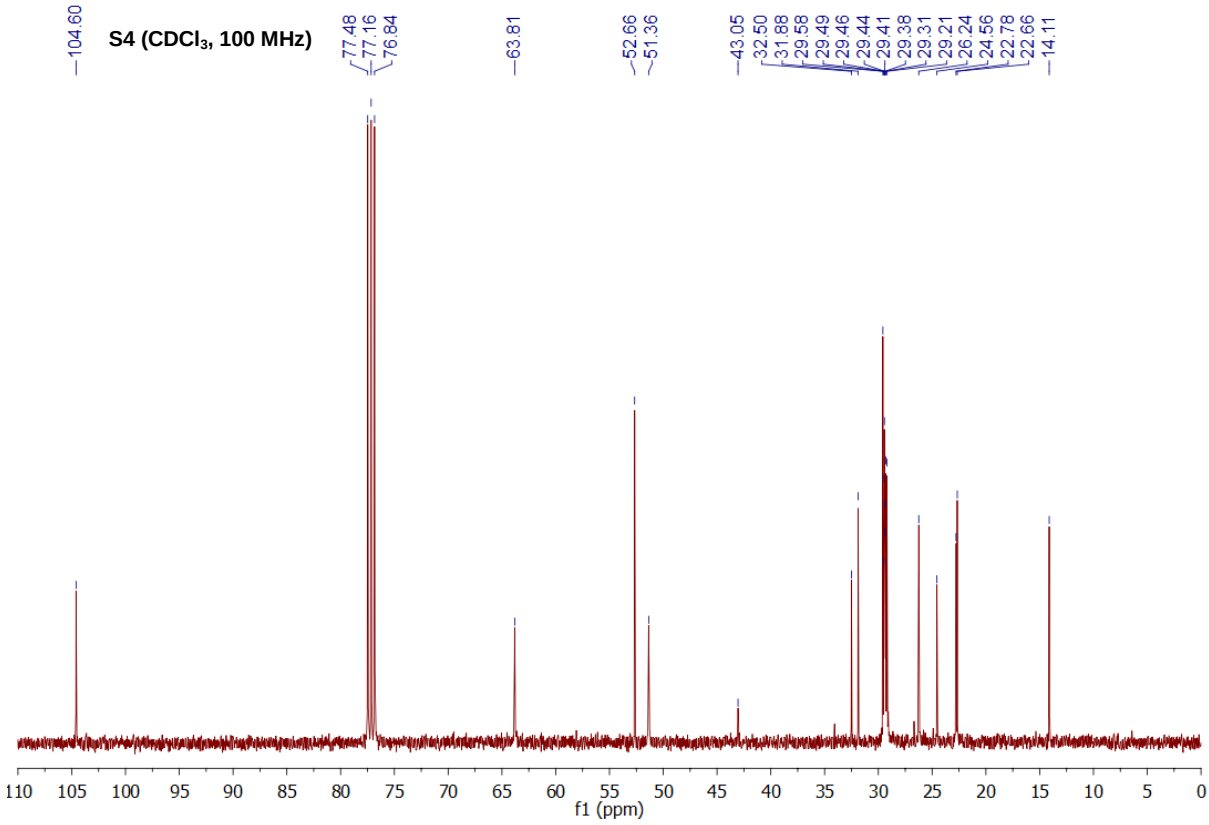

S5 ($CDCl_3$, 100 MHz)

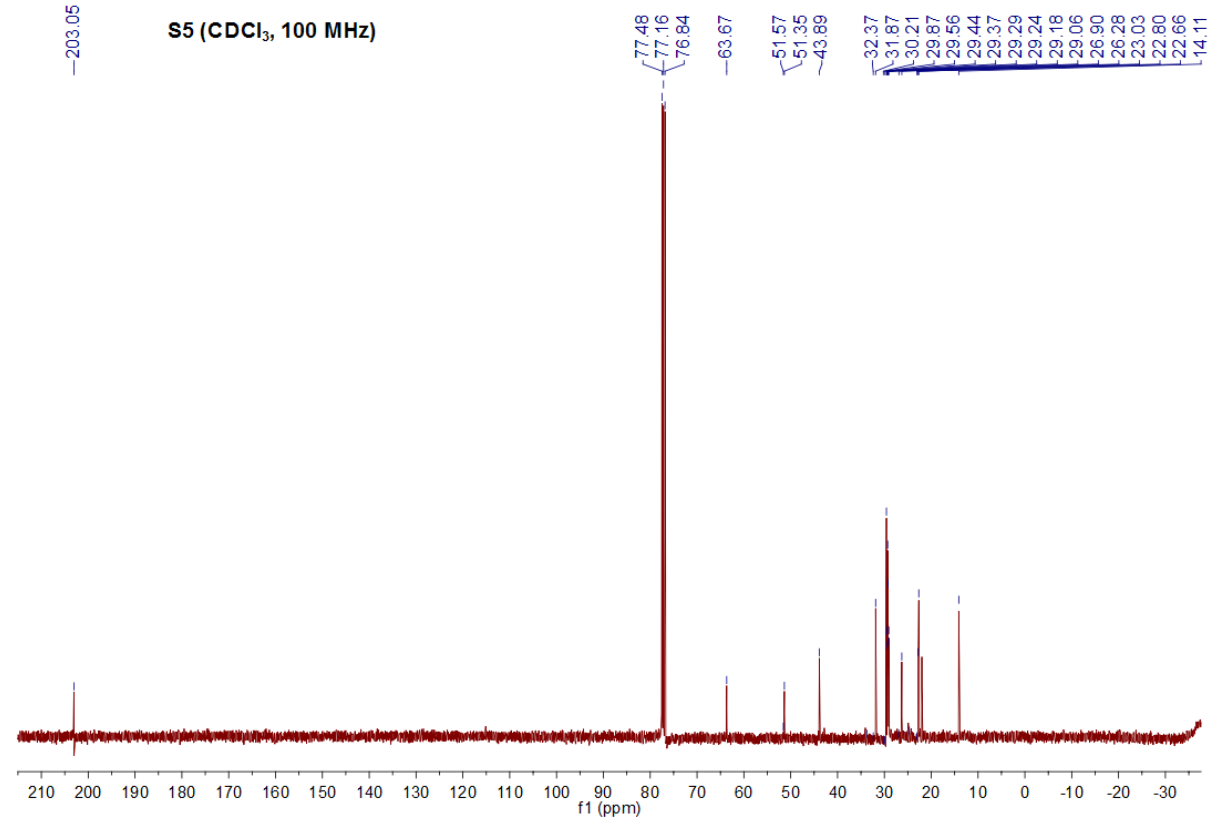

4. Procedures for the formation of vesicles

Lipid **1** (2 mg, 4.6 mmol) was added to HPLC grade water (1 mL) to give an aqueous suspension (4.6 mM). An amine (1 or 5 eq.) was added into the suspension, followed by bath sonication for 15 minutes giving a translucent suspension.

5. NMR spectra of suspension of hexyliminolipid (3e) in D_2O

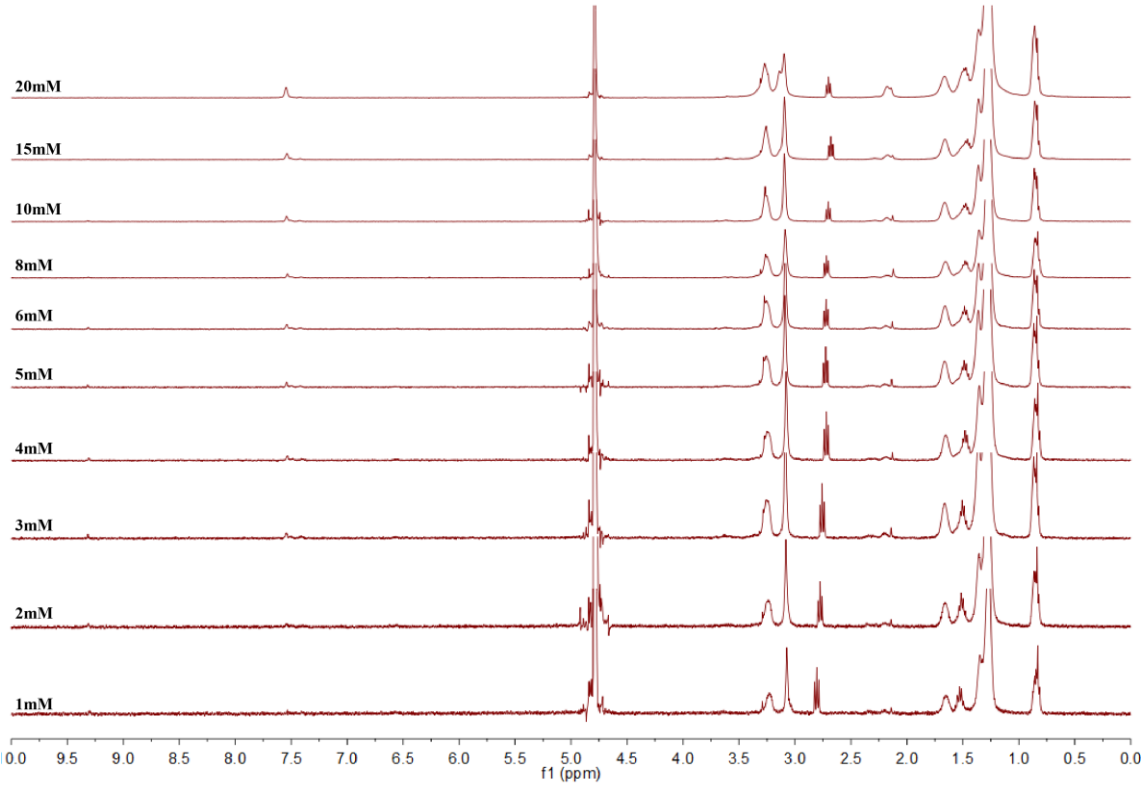

Figure S1. NMR trace of different concentration of iminolipid **3e** in D_2O.

Different concentrations (1 mM – 20 mM) of lipid **1** suspended in D_2O were prepared at room temperature. *n*-Hexylamine (**2e**, 1 eq.) was added into each suspension to give suspensions of **3e** at different concentrations. Each sample was the bath sonicated for 15 minutes at room temperature to give a translucent suspension, then the ^1H NMR spectra recorded after 2 hours (Figure S1).

The ^1H NMR spectra of a series of suspension of **3e** showed the complete disappearance of the aldehyde resonance of lipid **1** at 9.7 ppm (the small peak at 9.3 ppm is not due to the starting aldehyde lipid), the appearance of a weak and broad signal at ca. 7.5 ppm and a 0.5 ppm downfield shift in the broadened resonance of the methylene adjacent to the nitrogen (compared to hexylamine); these observations are consistent with imine formation. The lipid peaks were

significantly broadened from 1 mM to 20 mM, with a slight increase in broadening at the higher concentrations.

6. NMR spectrum of suspension of methyliminolipid (3a) in D_2O

The ^1H NMR spectrum of the mixture of DDAB-CHO **1** with methylamine **2a** in D_2O showed the presence of unreacted aldehyde **1** (peak at 9.3 ppm) with no imine visible.

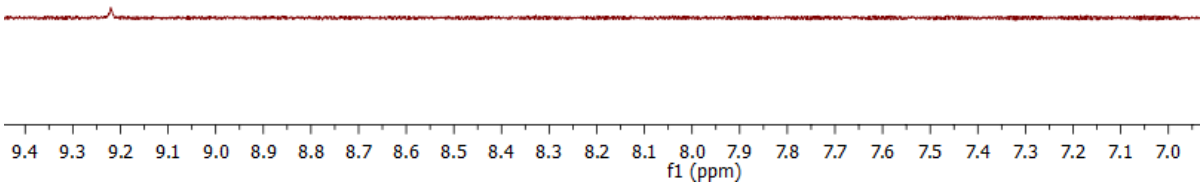

Figure S2. Partial NMR spectrum of iminolipid **3a** in D_2O (4.6 mM with 1 eq. methylamine).

7. Nile Red fluorescence emission spectra

All samples contained the Nile Red probe at a 1 µM concentration and were excited at 550 nm. All samples were freshly prepared at room temperature, followed by sonication for 15 minutes. The resulting suspensions were incubated at room temperature for 1 hour before the Nile Red emission was measured.

7.1 Example procedure for sample measurement

Three samples ((a), (b) & (c)) were prepared comprising: (a) HPLC water with Nile Red only; (b) suspension of 4.6 mM DDAB-CHO (lipid **1**); (c) suspension of 4.6 mM DDAB-CHO with 5 eq. hexylamine. The fluorescence emission spectra (ex. 550 nm) were recorded for each. Nile Red maximum emission of sample (a) was at 652 nm. A blue shift of 14 nm was observed for sample (b) (638 nm), indicating micelle formation. Blue shifted emission occurred at 627 nm for sample (c), a value that was consistent with the formation of bilayer-containing structures like vesicles.[3]

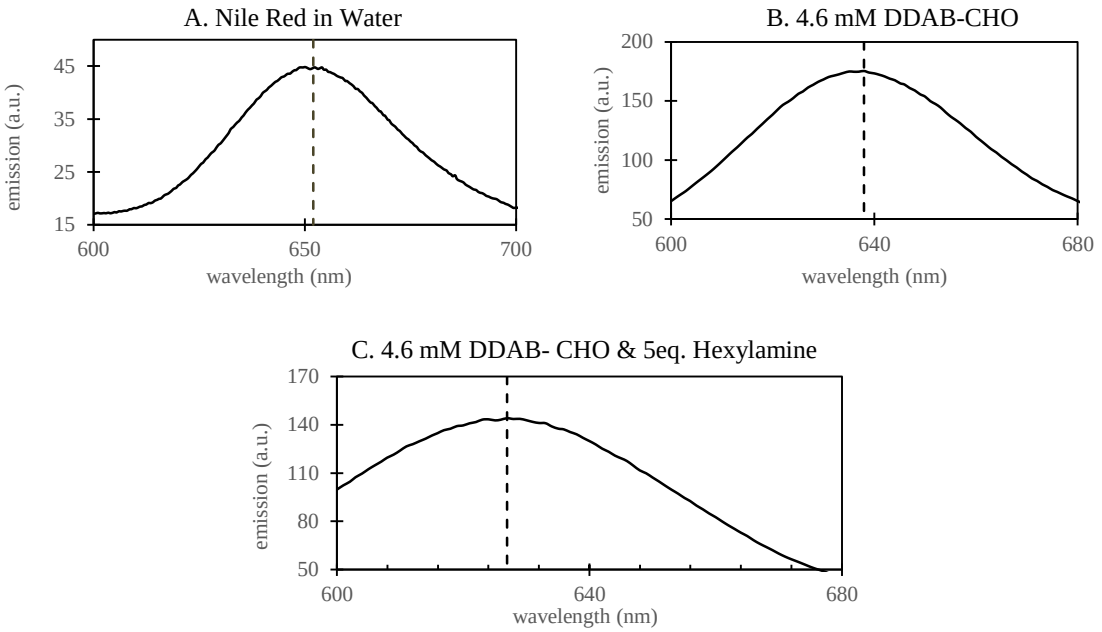

Figure S3. Nile Red fluorescence emission spectra of, (A) only in HPLC grade water; (B) lipid **1** (4.6 mM) suspension; (C) a mixture of lipid **1** (4.6 mM) with 5 eq. hexylamine.

7.2 Critical aggregation concentration (CAC) determinations for DDAB, lipid 1 and suspension of 3e

The procedure used was a modification of that described by van Esch.[3b] Samples of DDAB were prepared by successive dilution of a 10 mM stock suspension in HPLC grade water. The final pH was 4.8 ± 0.2. Each sample was sonicated for 15 mins before measurement of the fluorescence spectrum. The Nile Red emission maximum is plotted against a logarithmic concentration scale, and the CAC is given by the intercept of the two linear regions (Figure S4), where Nile Red emission significantly deviates from emission in water (652 ± 2 nm). Upper and lower bounds were estimated from the data. DDAB was used as a comparison and the CAC values obtained were similar to other publications.

For DDAB-CHO, samples were prepared by dissolving lipid **1** (DDAB-CHO) into HPLC grade water (pH 4.5 ± 0.5), followed by sonication for 15 mins and incubation for 2 hours at room temperature. For the *n*-hexyliminolipid, samples were prepared by dissolving lipid **1** (DDAB-CHO) and 1 eq. hexylamine into HPLC grade water (pH 10.8 ± 0.1), sonicated for 15 mins. The CAC was determined for these samples by the same method as mentioned above for the DDAB samples.

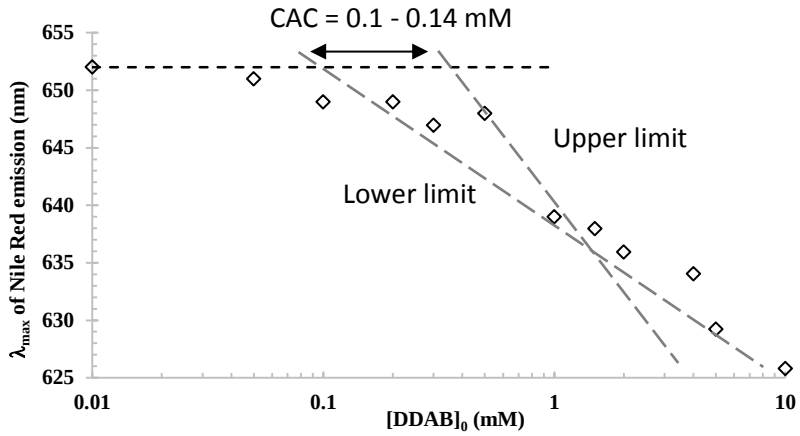

Figure S4. CAC (0.1 to 0.14 mM) determination of **DDAB** by fluorescence spectroscopy in HPLC grade water.

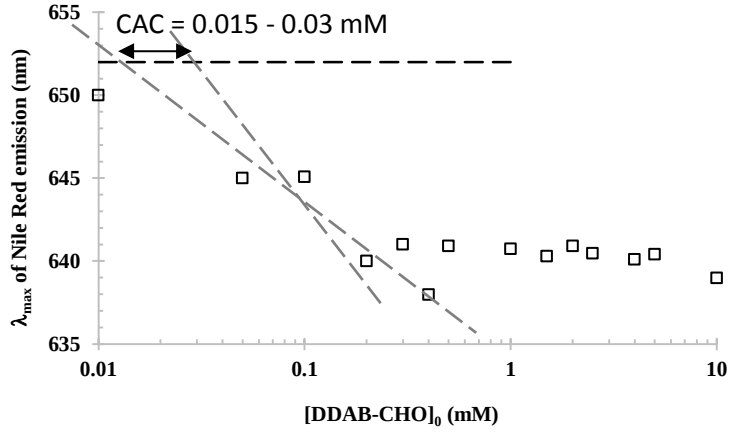

Figure S5. CAC (0.015 to 0.03 mM) determination of **DDAB-CHO** (lipid **1**) by fluorescence spectroscopy in HPLC grade water.

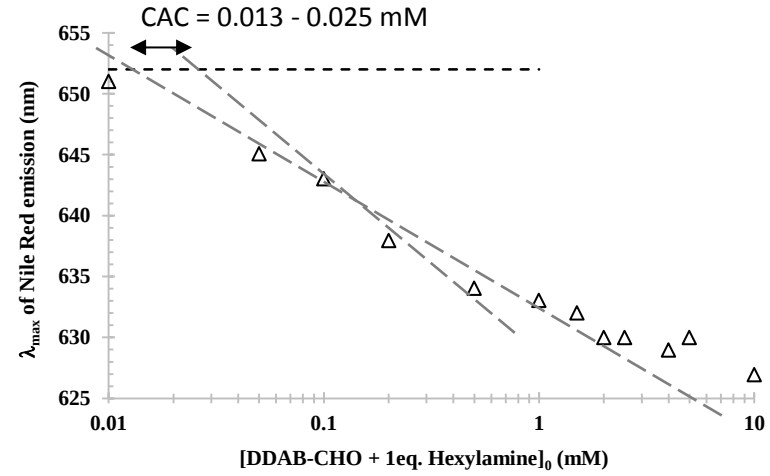

Figure S6. CAC (0.013 to 0.025 mM) determination of **DDAB-CHO** (lipid **1**) with 1 eq. hexylamine by fluorescence spectroscopy in HPLC grade water.

8. Dynamic light scattering (DLS) procedures and data

Dynamic light scattering measurements were performed on a Malvern Zetasizer Nano S (He-Ne laser 633 nm) instrument. The machine was calibrated using a polystyrene latex standard. Each sample (1 mL) was loaded into a disposable cuvette. DLS was performed at 25 °C at a backscatter angle of 173° with an equilibration time of 120 s, and 3 cycles were performed.

8.1 Example procedure for sample measurement

Lipid **1** and hexylamine were mixed in HPLC grade water (pH 10.8 ± 0.1 due to added amine) at a concentration of 4.6 mM lipid **1** and 1 eq. *n*-hexylamine, sonicated for 15 mins. The resulting suspension was incubated at room temperature for 1 hour before the sample was assayed. Measurements were performed at 25 °C. The polydispersity index (PDI) was measured as 0.398, which is relatively high compared to sonicated suspensions of phosphatidylcholines, which can have PDI values from 0.10 to 0.36 depending upon sonication power and lipid concentration.[4]

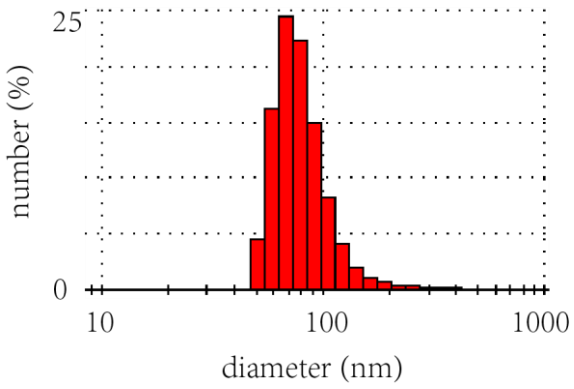

Figure S7. DLS data for 4.6 mM DDAB-CHO with 1 eq. hexylamine sample. The sample was measured three times, and the majority of self-assembled structures were from 50 to 90 nm in diameter.

9. Encapsulation study procedures and data

Rhodamine B (95.8 mg, 0.2 mmol) was dissolved in HPLC grade water (100 mL), giving a 2 mM rhodamine B stock solution (always stored protected from light). The lipid to be studied (e.g. DDAB or lipid **1**, 5 mg, with 1 eq. hexylamine) was added to an aliquot of this stock solution (2.5 mL) and the suspension (4.6 mM lipid) was bath sonicated for 15 mins to form vesicles. The samples were left for 2 hours before the non-encapsulated dye (rhodamine B) was removed by GPC (gel permeation chromatography) using PD-10 desalting columns containing Sephadex G-25 medium (size exclusion limit M_r = 5,000 Da). The column storage solution (0.15 % Kathon) was discarded, which was followed by equilibriation of the column with HPLC grade water (30 mL). Then each vesicle

suspension (2.5 mL) was added to the column and the first eluted fraction discarded. Then, the column was eluted with HPLC grade water (3.5 mL) and the collected eluent was assayed by UV-visible spectrophotometry.

The UV-visible spectra (200 - 700 nm) of the post-GPC suspensions (2 mL) were collected using Sigma brand spectrophotometer silica (quartz) cuvettes with 10 mm path lengths. Data were recorded on an Agilent Technologies Cary 60 UV-Visible spectrometer (600 nm/min) with three cycle counts (0.1 min/cycle).

To calculate encapsulation efficiency of RhB in the vesicles (**Fig. S8**):

- RhB stock solution (2 mM, 4 µL) was added to 2 mL HPLC grade water to give a 4 µM solution and the absorbance at the λ_{max} was measured. The absorbance was:

$$A_{RhB}\ (\lambda_{554}) = 0.429$$

- The absorbance of RhB when mixed with DDAB (4.6 mM) and DDAB-CHO (4.6 mM) was shifted by ca. 30 nm.

$$A_{RhB\ in\ DDAB}\ (\lambda_{524}) = 0.144$$

$$A_{RhB\ in\ DDAB\text{-}CHO}\ (\lambda_{527}) = 0.151$$

(1) For DDAB, taking into account the 1.4-fold dilution from the GPC column:

$$\left(\frac{3.5}{2.5}\right) \times \left(\frac{0.144}{0.429}\right) \times \left(\frac{4 \times 10^{-6}\ \mathrm{M}}{2 \times 10^{-3}\ \mathrm{M}}\right) \times 100 = 0.09\ \%$$

(2) For lipid **1**, the calculation method was the same with DDAB (above),

$$\left(\frac{3.5}{2.5}\right) \times \left(\frac{0.151}{0.429}\right) \times \left(\frac{4 \times 10^{-6}\ \mathrm{M}}{2 \times 10^{-3}\ \mathrm{M}}\right) \times 100 = 0.10\ \%$$

(3) For lipid **1** with 1 eq. hexylamine (**2e**), $A_{DDAB\text{-}CHO}\ (\lambda_{525}) = 0.407$

$$\left(\frac{3.5}{2.5}\right) \times \left(\frac{0.407}{0.429}\right) \times \left(\frac{4 \times 10^{-6}\ \mathrm{M}}{2 \times 10^{-3}\ \mathrm{M}}\right) \times 100 = 0.27\ \%$$

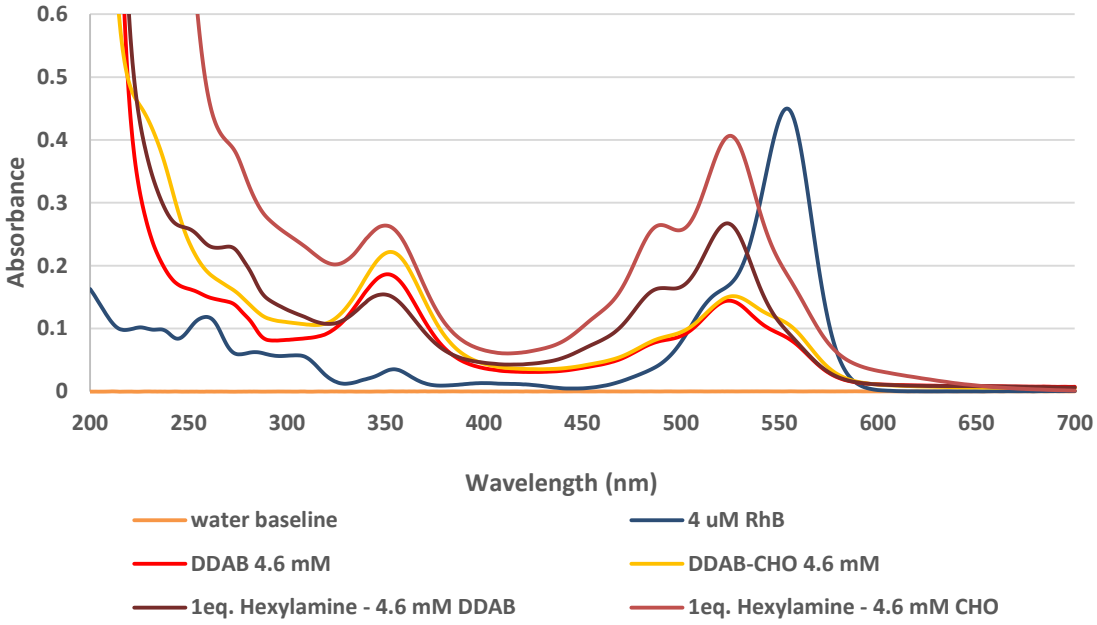

Figure S8. Example of UV absorbance data from the encapsulation studies.

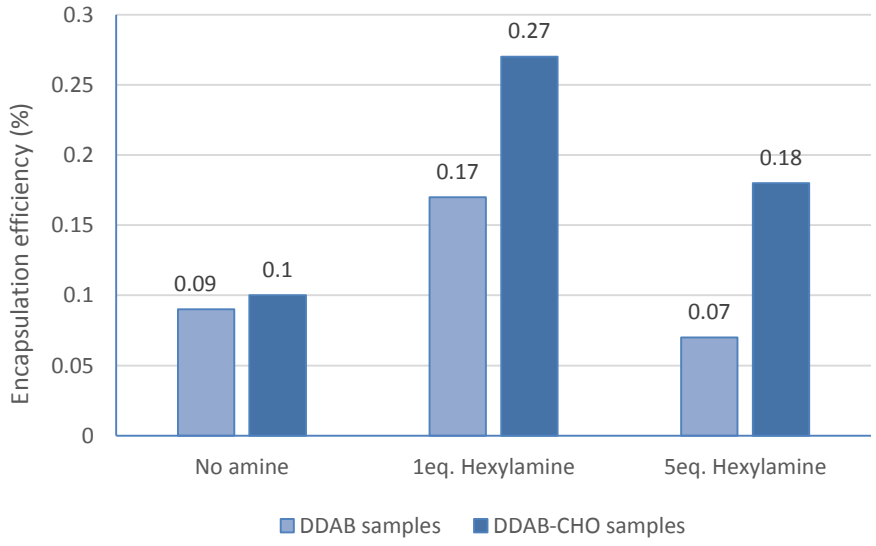

Figure S9. Collated RhB encapsulation studies for DDAB/lipid **1** with hexylamine.

10. TEM and SEM procedures and images

10.1 TEM

Images were obtained on a Phillips CM20 electron microscope operating at 200 kV. Samples were prepared by depositing drops of aqueous mixture (4.6 mM DDAB-CHO with 1 eq. hexylamine, followed sonication for 15 mins and two hours of incubation at room temperature) onto the formvar

coated carbon grid of mesh size 200 (Agar scientific, Formvar/Carbon 200 mesh Cu (50), thin cast films of Formvar strengthened with the addition of a layer of evaporated carbon on copper grids). The excess liquid was blotted away (filter paper). The grids were allowed to dry at room temperature overnight. Micrographs (e.g. Figure S10) were recorded on a CCD camera.

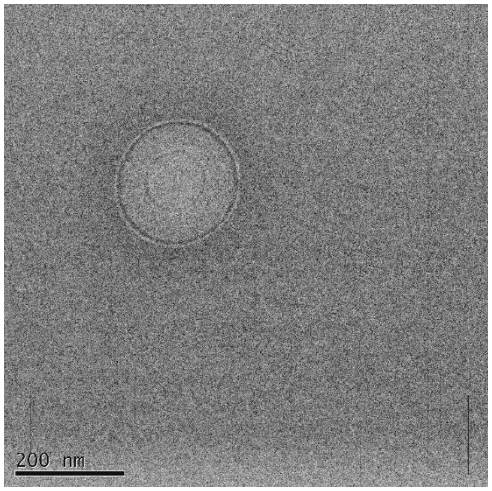

Figure S10. Transmission electron microscopy image of a vesicle-in-vesicle observed from a suspension of lipid **2e** in water.

10.2 SEM

Scanning electron microscopy was performed with a FEI Quanta 650 FEG-(E) SEM instrument. The samples were prepared by drop casting the solution (4.6 mM lipid **1** with 1 eq. amine) onto the specimen stubs (Agar Scientific, 12.5 mm dia, 3.2 × 8 mm pin) surface. The surface was allowed to dry at room temperature overnight. All samples were imaged coated with gold (10-15 nm).

SEM images of suspensions of **3e** (Figure S11, (D)) showed spherical structures with sizes generally between 0.15 and 1.0 μm (majority 0.25 to 0.8 μm). These spherical objects, which are probably vesicles, are different in size to those measured by DLS, and it is suggested that air-drying of the suspension during preparation of the samples for SEM may have caused the vesicles to fuse into up to micron-sized vesicles (GUVs). Imaging of suspensions of **3a** (Figure S11, (A)) treated in an identical way showed no structures that resembled vesicles. Imaging of suspensions of **3b** (Figure S11, (B)) treated in an identical way showed some vesicle-like structures, although the size is variable and the surface is relatively uneven. Imaging of suspensions of **3p** (Figure S11, (C)) treated in an identical way showed vesicle-like structures.

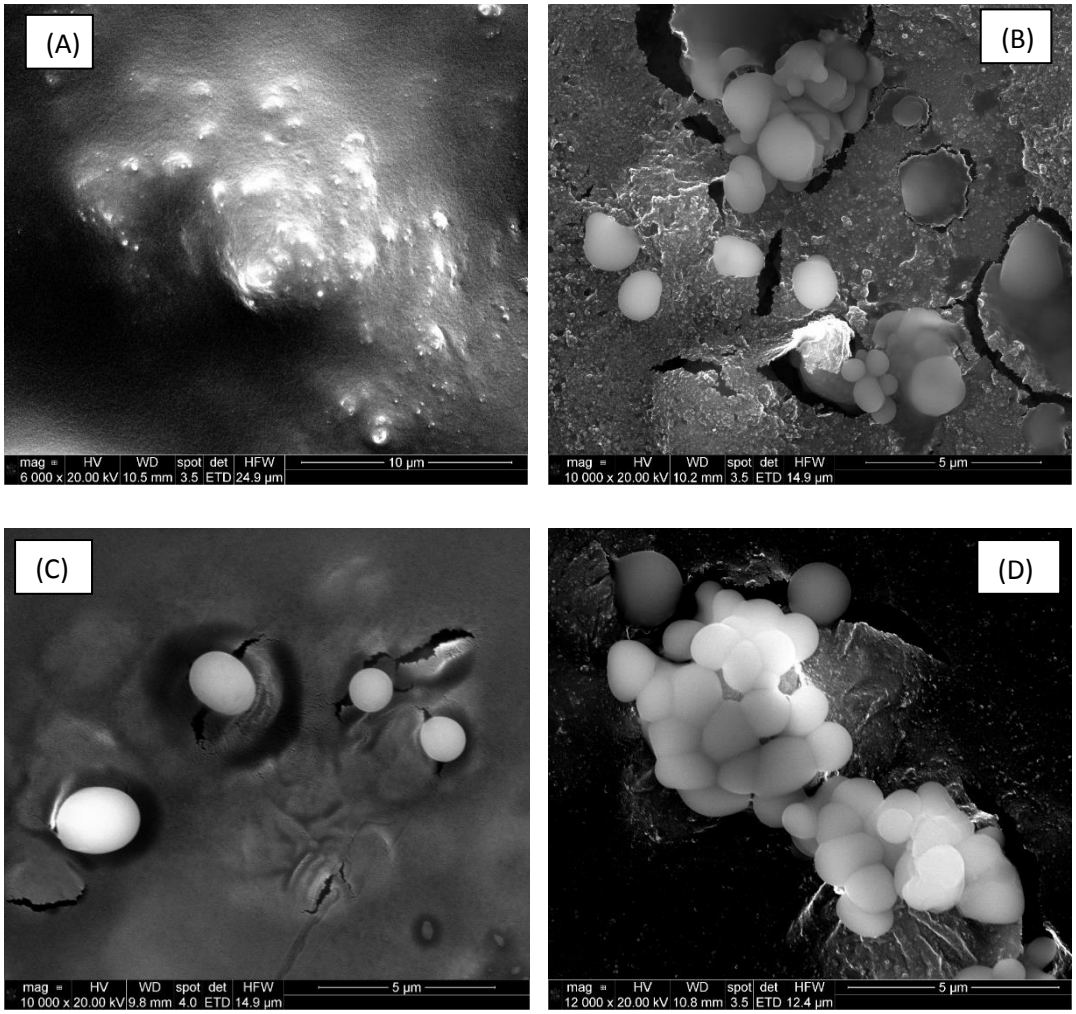

Figure S11. Scanning electron microscopy images of dried suspensions of (A) **3a**, (B) **3b**, (C) **3p** and (D) **3e**.

11. Differential scanning calorimetry (DSC) procedures and thermograms

Measurements were performed on a Diamond DSC (PerkinElmer), equipped with 100 µL twin cells. The twin cells were filled with the sample (1.350 mg, paste of 8.7 mg lipid **1** with 1 eq. hexylamine in 20 µL water) and the reference (HPLC grade water). Standard 4.6 mM samples were too dilute to obtain suitable data. The DSC thermograms of the samples were obtained at a scanning rate of 5 °C/min for both heating (from 0 °C to 100 °C) and cooling (from 100 °C to 5 °C) scan. A weak exotherm was observed at ca. 10 °C on the heating cycle, but the cooling cycle gave an endotherm with onset at 11 °C. By comparison to the literature data for DDAB,[5] this transition was ascribed to the melting temperature (T_m) of a bilayer.

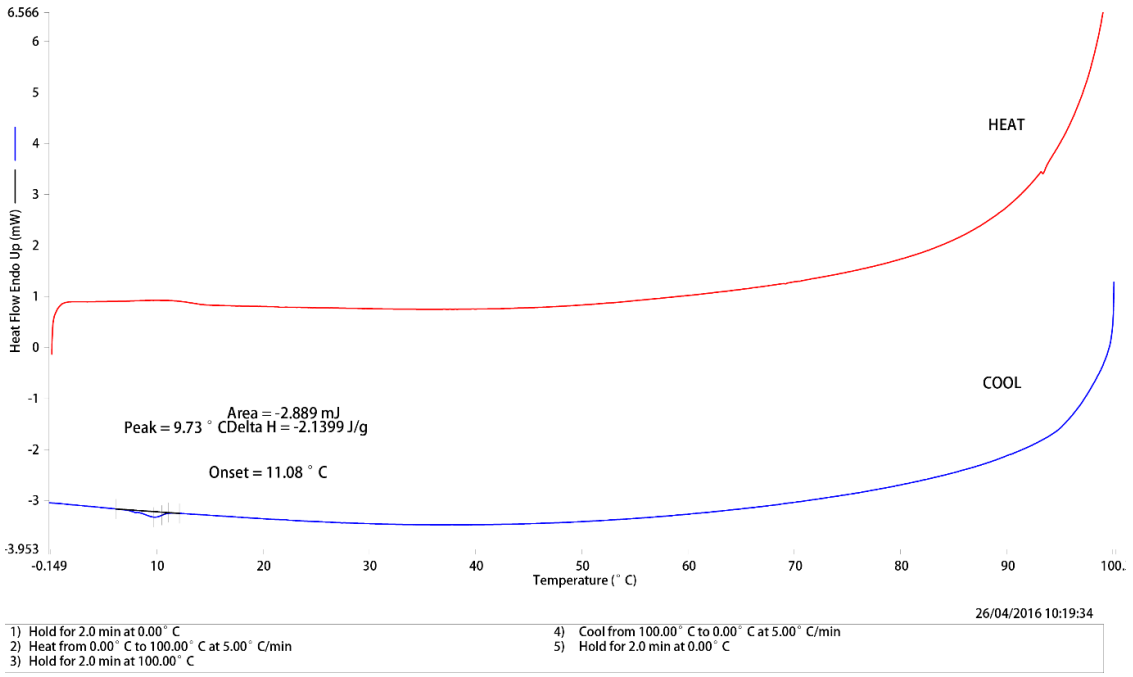

Figure S12. DSC trace of the paste of lipid **1** with 1 eq. hexylamine. Endotherm with onset at 11°C shown.

12. HPLC-MS procedures and data

The exchanging imine mixtures of **3e**/**3a** and **3e**/**3b** were analyzed by HPLC-MS after reduction to the amines by $NaBH_3CN$. The samples were prepared by mixing lipid **1** (2 mg, 4.6 mM) with 1 eq. methylamine **2a** or *n*-propylamine **2b** in water (1 mL), then adding another 1 eq. of *n*-hexylamine **2e**. The sample without *n*-hexylamine (**1** with **2a**/**2b** only) was also assayed as a comparison. Each suspension was incubated for 2 hours, then the equilibrated mixture was "fixed" by addition to $NaBH_3CN$ (~ 240 mM after mixing, 3 mg in 0.2 mL mixture). The "fixed" samples were diluted with another 0.8 mL MeOH to meet the concentration requirements of the HPLC-MS, and analyzed using 50 % H_2O (with 0.1% TFA V/V) and 50 % ACN. The peaks of many amines produced were not UV-visible active, so had to be identified by mass spectrometry (ESI-MS). The area peak on a mass spectrum does not is an indicative but not quantitative measure of the proportions of these very structurally similar compounds. However, for the same compound, bigger area means larger amount of this compound if compared with different spectra.

HPLC-MS analysis of the mixture of hexylamine, lipid **1** and methylamine showed the amount of reduced methyliminolipid **3a** had decreased compared to the mixture of lipid **1** and methylamine (Figure S13a). Similar changes were observed for the mixture of hexylamine, lipid **1** and propylamine, which showed the amount of reduced propyliminolipid **3b** had decreased compared to the sample with only lipid **1** and propylamine (Figure S13b). HPLC-MS assays of the reverse addition

of methylamine/propylamine to a mixture of **1** and hexylamine (Figure S13c,d) showed the amount of reduced hexyliminolipid **3e** formed did not change significantly.

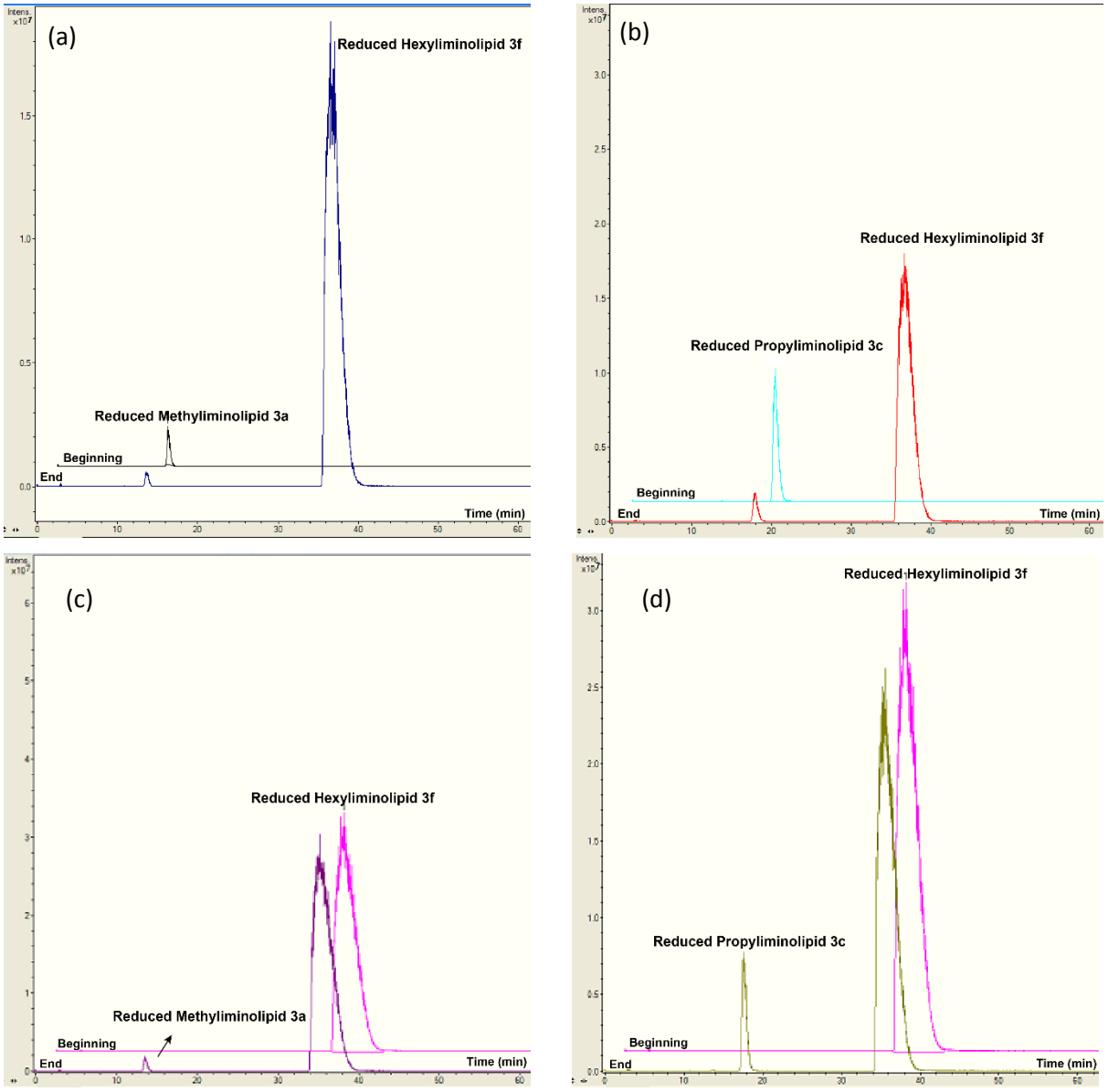

Figure S13. (a,b) LCMS analyses of mixtures of (a) *n*-hexylamine, lipid **1** and methylamine and (b) *n*-hexylamine, lipid **1** and *n*-propylamine. (c,d) LCMS analyses of mixtures formed by the reverse addition of (c) methylamine to a mixture of lipid **1** and *n*-hexylamine and (d) *n*-propylamine to a mixture of lipid **1** and *n*-hexylamine.

13. Procedure for the determination of K_{rel} and NMR spectra

Exchange reactions between amines and iminolipids were monitored by ^{1}H NMR. The spectra were recorded at 25 °C on a Bruker DPX spectrometer (at 400 MHz), with an internal deuterium lock. Two reference solutions were freshly prepared each time by mixing 4.6 mM **1** with 1 eq. benzylamine in $CDCl_3$ or mixing 4.6 mM **1** with 1 eq. benzylamine in D_2O with sonication for 15 mins, respectively (solvent volume = 0.7 mL). Then to establish an equilibriating mixture, the amine of interest (1 eq.) was added into the stock solutions. ^{1}H NMR spectra were recorded after incubation of the samples at room temperature for 2 hours. For the D_2O samples, MeOH (0.4 μL) was added into each NMR sample (0.7 mL D_2O) as an internal integration standard. The internal standard permitted calculation of relative exchange constants K_{rel} in D_2O, as the imine peaks were significantly broadened.

The key equilibria are:

$$\mathrm{R^1NH_2} + \mathrm{DDAB\text{-}CHO} \rightleftharpoons \mathrm{R^1N{=}CH\text{-}DDAB} + \mathrm{H_2O} \quad (1)$$

$$\mathrm{R^2NH_2} + \mathrm{DDAB\text{-}CHO} \rightleftharpoons \mathrm{R^2N{=}CH\text{-}DDAB} + \mathrm{H_2O} \quad (2)$$

As $[H_2O]$ = constant,

$$K_1 = {[\mathrm{R^1N = CH - DDAB}]}/{[\mathrm{R^1NH_2}][\mathrm{DDAB - CHO}]} \quad (3)$$

$$K_2 = {[\mathrm{R^2N = CH - DDAB}]}/{[\mathrm{R^2NH_2}][\mathrm{DDAB - CHO}]} \quad (4)$$

In general the amount of free aldehyde was low, comprising 0.05 $\pm$ 0.02 mol% of the mixture in $CDCl_3$ and 0.04 $\pm$ 0.03 mol% in D_2O. The relative equilibrium constant was given by:

$$K_{rel} = \frac{K_2}{K_1} = \frac{[\mathrm{R^2N{=}CH{-}DDAB}][\mathrm{R^1NH_2}]}{[\mathrm{R^1N{=}CH{-}DDAB}][\mathrm{R^2NH_2}]} \quad (5)$$

13.1 Reactions in $CDCl_3$

After the amine of interest had been added to the reference solution in $CDCl_3$, resonances due to all four components (Equation **(5)**) could be identified in each ^{1}H NMR ($CDCl_3$) spectrum at equilibrium. Since the volume is fixed the concentration are all proportional to the normalised integration values for each compound. For instance, the spectrum of exchange reaction between benzylamine and hexylamine (R^1 = benzylamine; R^2 = *n*-hexylamine) in $CDCl_3$ is shown below (**Fig. S14**):

$$K_{rel} = \frac{[hexyl{-}imine][benzyl{-}amine]}{[benzyl{-}imine][hexyl{-}amine]} = \frac{1.271 \times {}^{4.395}/_{2}}{1.000 \times {}^{3.501}/_{2}} = 1.596$$

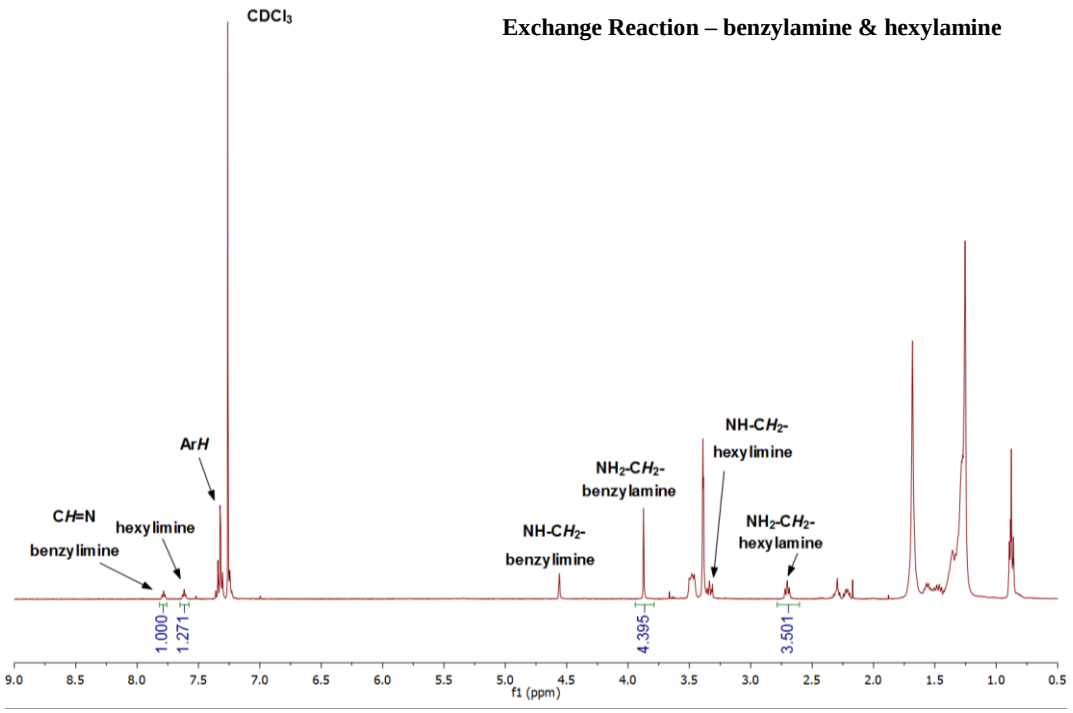

Figure S14 ^{1}H NMR spectrum of mixture of benzylamine and hexylamine with lipid **1** in $CDCl_3$.

The same method of calculation was applied to the other samples. Measurements on each pair of amines were completely three times. One representative NMR spectrum for each pair of amines is shown in Section 13.3. The relative exchange constant (K_{rel}) will be displayed as [average±SD], and is shown in **Table S1**.

Table S1. Relative exchange constants obtained (K_{rel}) for a series of amines added to benzyl iminolipid vesicles in $CDCl_3$.

Amine	Sample 1	Sample 2	Sample 3	Exchange constant (K_{ex}) in $CDCl_3$	clogP
Methylamine	2.910	2.982	2.877	2.92 ± 0.05	-0.664
n-Propylamine	1.379	1.343	1.442	1.39 ± 0.05	0.394
2-Methylpropylamine	1.614	1.578	1.555	1.58 ± 0.03	0.793
3-Azidopropylamine	1.560	1.536	1.652	1.58 ± 0.06	0.851
n-Butylamine	1.554	1.584	1.488	1.54 ± 0.05	0.923
Benzylamine	1.0	1.0	1.0	1.0	1.094
2,2-Dimethylpropylamine	1.543	1.510	1.540	1.54 ± 0.03	1.192
3-Methylbutylamine	1.493	1.405	1.488	1.46 ± 0.05	1.322
Cyclohexylamine	0.565	0.557	0.536	0.55 ± 0.02	1.367
Aminomethylcyclopentane	1.408	1.353	1.475	1.41 ± 0.06	1.427
n-Pentylamine	1.572	1.444	1.498	1.50 ± 0.06	1.452
3,3-Dimethylbutylamine	1.533	1.486	1.500	1.51 ± 0.02	1.721
n-Hexylamine	1.557	1.596	1.587	1.58 ± 0.02	1.981
1-Naphthylmethylamine	1.011	1.10	1.050	1.05 ± 0.06	2.268
n-Heptylamine	1.47	1.360	1.403	1.41 ±0.06	2.510
n-Octylamine	1.554	1.446	1.402	1.47 ±0.08	3.039
Pyrenemethylamine	1.328	1.191	1.109	1.21 ±0.11	3.902
n-Decylamine	1.510	1.505	1.547	1.52 ±0.02	4.097

13.2 Reactions in D_2O

After the second amine as added in D_2O, the two imine peaks of the four components needed in the equation **(5)** could not be accurately integrated due to their broadness. Therefore methanol (0.4 µL in 0.7 mL D_2O, 14.13 mM) was added into each NMR sample as an internal standard for integration that would allow calculation of exchange constants. Furthermore before addition of the amine of interest, the initial amount of free benzylamine in the reference sample, $[PhCH_2NH_2]_i$, was measured from the relative integration of the methylene resonance (compared to the 14.13 mM methanol standard). Any increase in the value of this integral (relative to the added MeOH) after addition of a new amine (RNH_2) would be ascribable to displacement of benzylamine from the benzyliminolipid.

Since both benzylamine and the benzyliminolipid have five phenyl protons, the integral from 7-7.3 ppm (which ***excludes*** the very weak imine N=CH resonances at 7.5-7.8 ppm) will give the combined concentrations of benzyl containing compounds. Since the final concentration of free benzylamine $[PhCH_2NH_2]_f$ can be calculated from the integration of the resonance due to the two methylene protons, then the relative concentration of the benzyliminolipid [$PhCH_2N$=CH-DDAB] can be calculated from the difference between these values after normalisation.

The concentration of the amine of interest, $[RNH_2]$, can be obtained directly from the ^1H NMR spectrum, but the concentration of the product iminolipid [RN=CH-DDAB] can only be inferred from the increase in the integral of free benzylamine after addition of RNH_2; the formation of RN=CH-DDAB resulted in equimolar displacement of benzylamine from the benzyliminolipid. Therefore:

$$[RN{=}CH\text{-}DDAB] = [PhCH_2NH_2]_f - [PhCH_2NH_2]_i \qquad \textbf{(6)}$$

Combining these values then gives the equilibrium constant K_{rel}. This can be exemplified with the integrals from the spectra recorded for the addition of *n*-hexylamine to a benzylamine/lipid **1** mixture.

(A) Integral for CH_2-N of $[PhCH_2NH_2]_i$ before *n*-hexylamine (direct from spectra, Fig. S15) = 0.214

(B) Integral for CH_2-N of $[PhCH_2NH_2]_f$ after *n*-hexylamine (direct from spectra, Fig. S16) = 0.250

(C) Integral for CH_2-N of $[CH_3(CH_2)_5NH_2]$ after n-hexylamine (from spectra, Fig. S16) = 0.222

(D) Integral for ArH for $[PhCH_2NH_2]_f$ + [$PhCH_2N$=CH-DDAB] after n-hexylamine (Fig. S16) = 0.703

(E) $[PhCH_2NH_2]_f$ comes from (D) – (B)

Therefore:

$$K_{rel} = \frac{K_2}{K_1} = \frac{[\mathrm{RN{=}CH{-}DDAB}][\mathrm{PhCH_2NH_2}]}{[\mathrm{PhCH_2N{=}CH{-}DDAB}][\mathrm{RNH_2}]} = \frac{(\frac{0.250}{2} - \frac{0.214}{2}) \times (\frac{0.250}{2})}{(\frac{0.703}{5} - \frac{0.250}{2}) \times (\frac{0.222}{2})} = 1.230$$

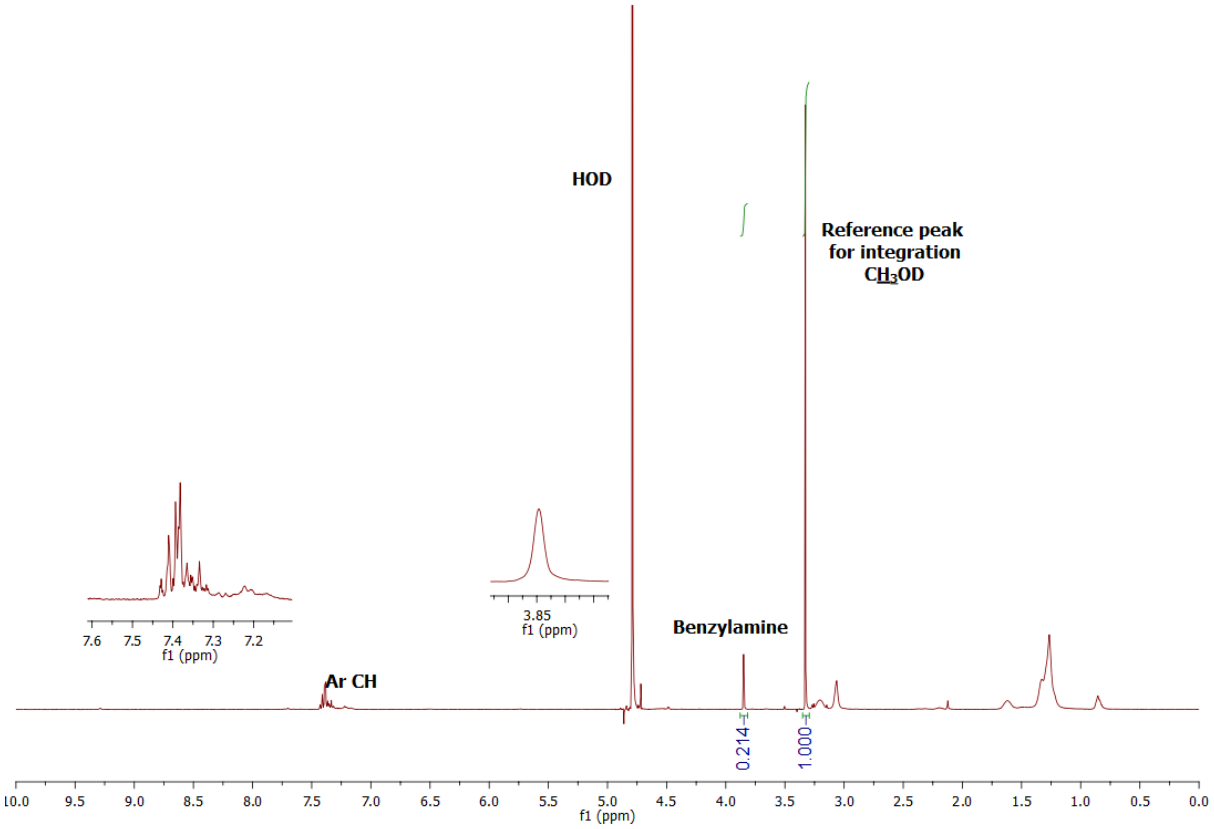

Figure S15. ^{1}H NMR spectrum of benzylamine with lipid **1** in D_2O.

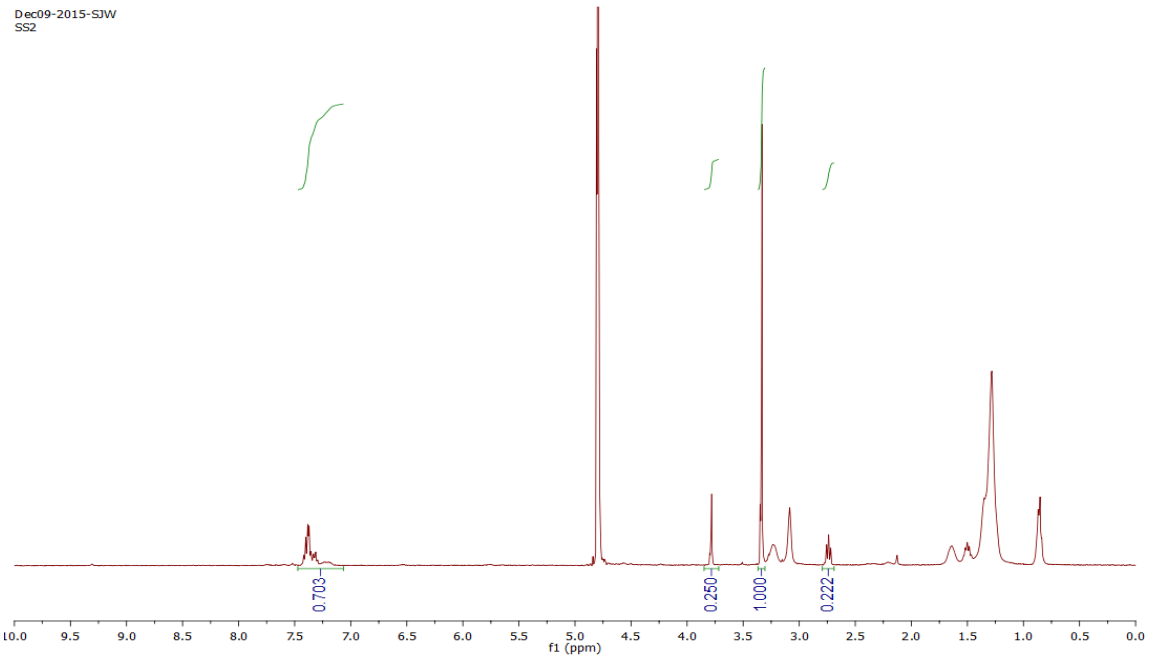

Figure S16. ^{1}H NMR spectrum of benzylamine with lipid **1** in D_2O after addition of *n*-hexylamine.

The exchange constant of several other amines were calculated using this method. As for measurements in $CDCl_3$, these measurements were repeated three times and an average obtained (Table S2).

Calculated logP values were calculated in ChemBioDraw Ultra 13.0. Specific algorithms for calculating LogP from fragment-based methods developed by the Medicinal Chemistry Project and BioByte. For more information, see http://www.biobyte.com/blqsar/index.html. These are averaged cLogP values from the following three estimation methods: Crippen's fragmentation, Viswanadhan's fragmentation, and Broto's method. The clogP value for 3-azidopropylamine was calculated by chemexper.com.

Table S2. The relative exchange constant of amines in D_2O.

Amine	K_{rel} **in** D_2O	**clogP**
Methylamine	0.13 ± 0.13	-0.664
n-Propylamine	0.23 ± 0.18	0.394
2-Methylpropylamine	0.20 ± 0.20	0.793
3-Azidopropylamine	0.13 ± 0.07	0.851
n-Butylamine	0.25 ± 0.15	0.923
Benzylamine	1.0	1.094
2,2-Dimethylpropylamine	0.85 ± 0.35	1.192
3-Methylbutylamine	0.18 ± 0.08	1.322
Cyclohexylamine	0.14 ± 0.06	1.367
Aminomethylcyclopentane	0.75 ± 0.25	1.427
n-Pentylamine	0.55 ± 0.15	1.452
3,3-Dimethylbutylamine	0.10 ± 0.10	1.721
n-Hexylamine	1.25 ± 0.25	1.981
1-Naphthylmethylamine	2.00 ± 1.00	2.268
n-Heptylamine	1.60 ± 0.40	2.510
n-Octylamine	1.25 ± 0.25	3.039
n-Decylamine	2.20 ± 1.00	4.097

13.3 NMR spectra in $CDCl_3$

Benzylamine - Methylamine

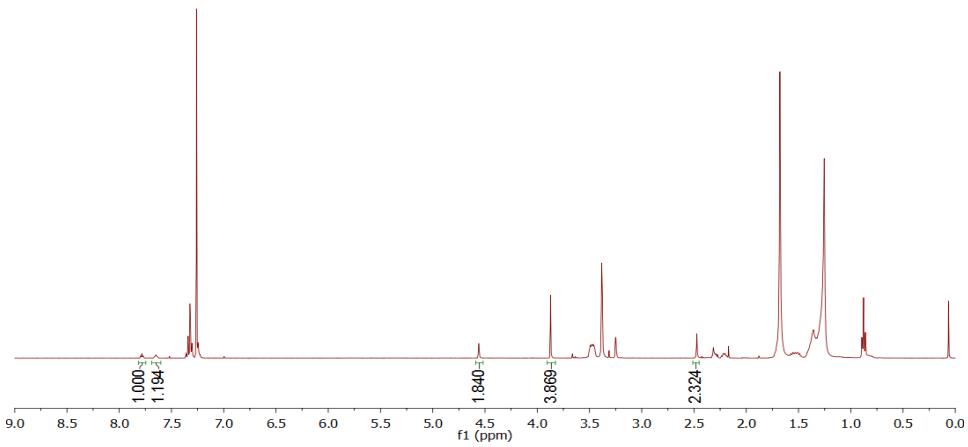

Benzylamine - Propylamine

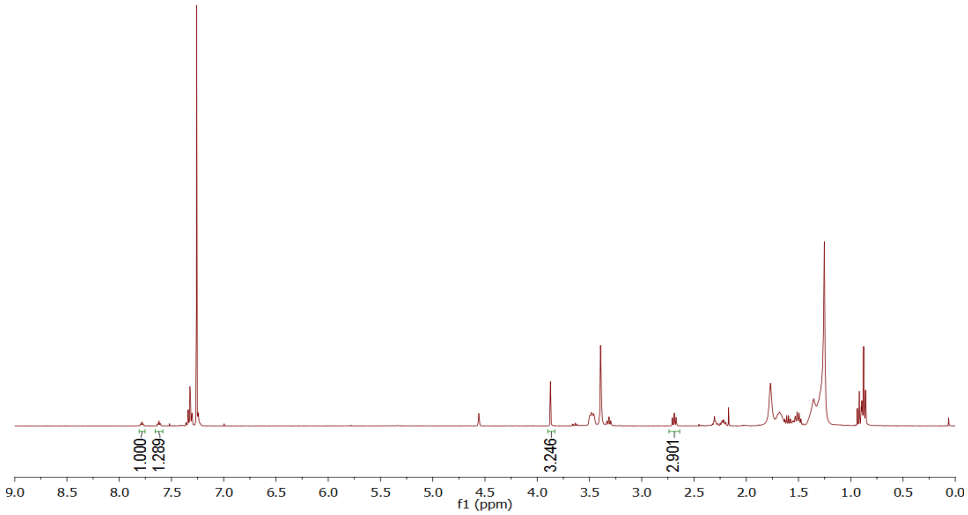

Benzylamine - 2-Methylpropylamine

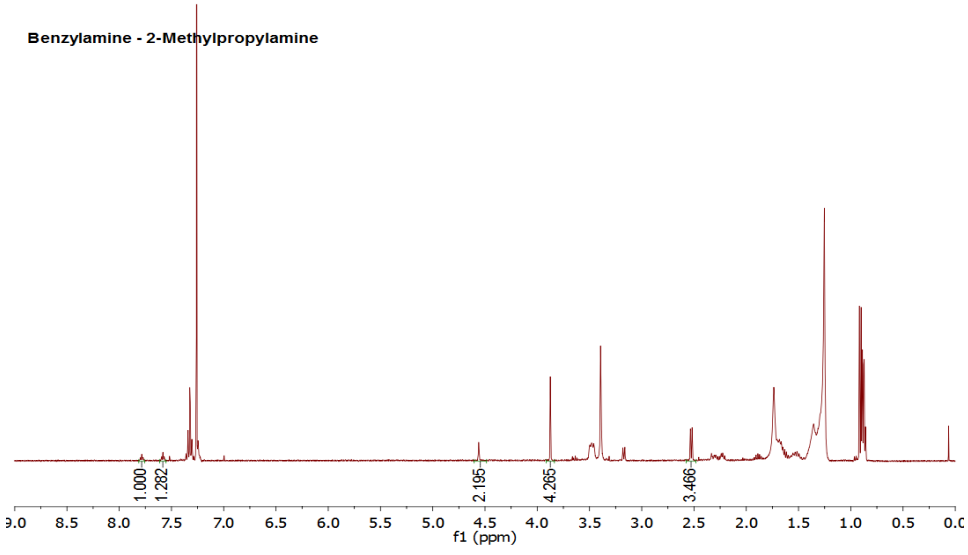

Benzylamine - 3-Azidopropylamine

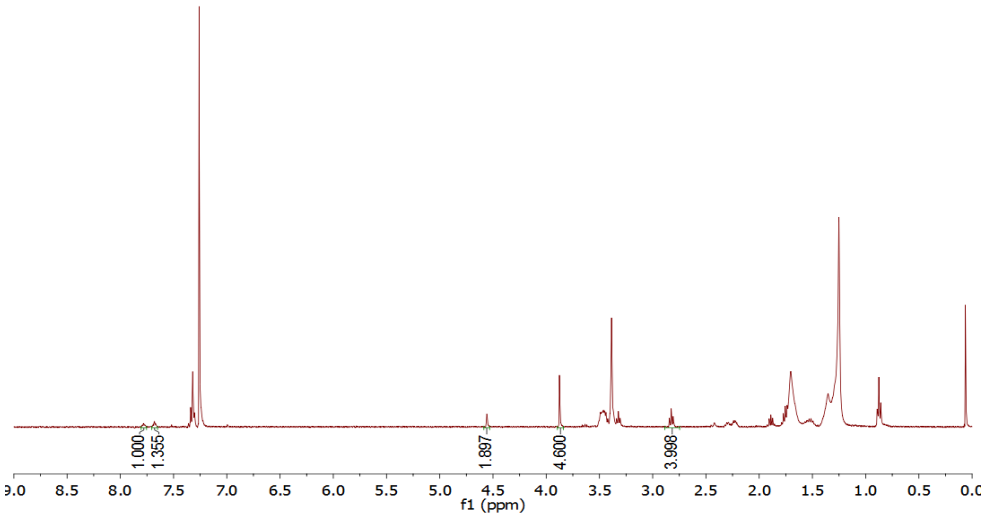

Benzylamine - 1-Butylamine

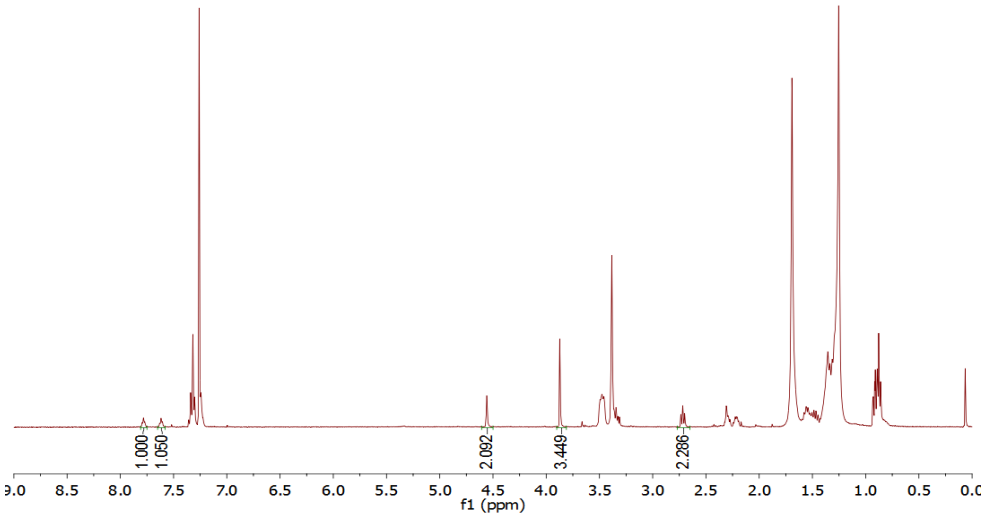

Benzylamine - 2,2-Dimethylpropylamine

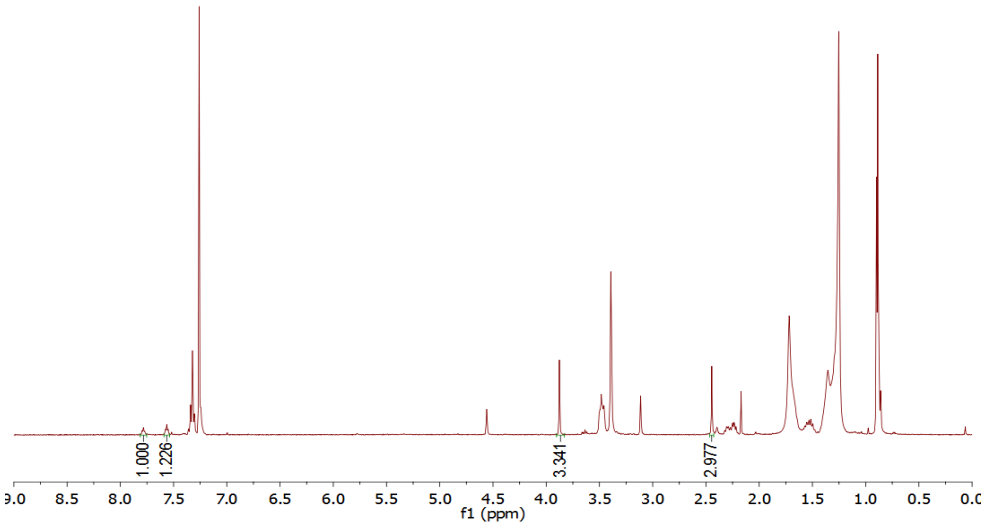

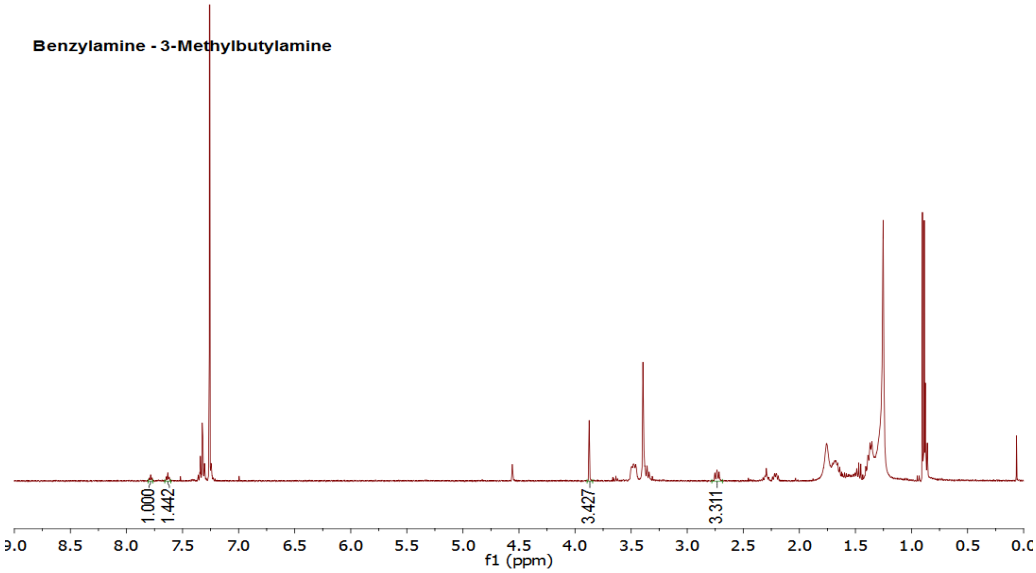
Benzylamine - 3-Methylbutylamine
1.000
1.442
3.427
3.311
f1 (ppm)

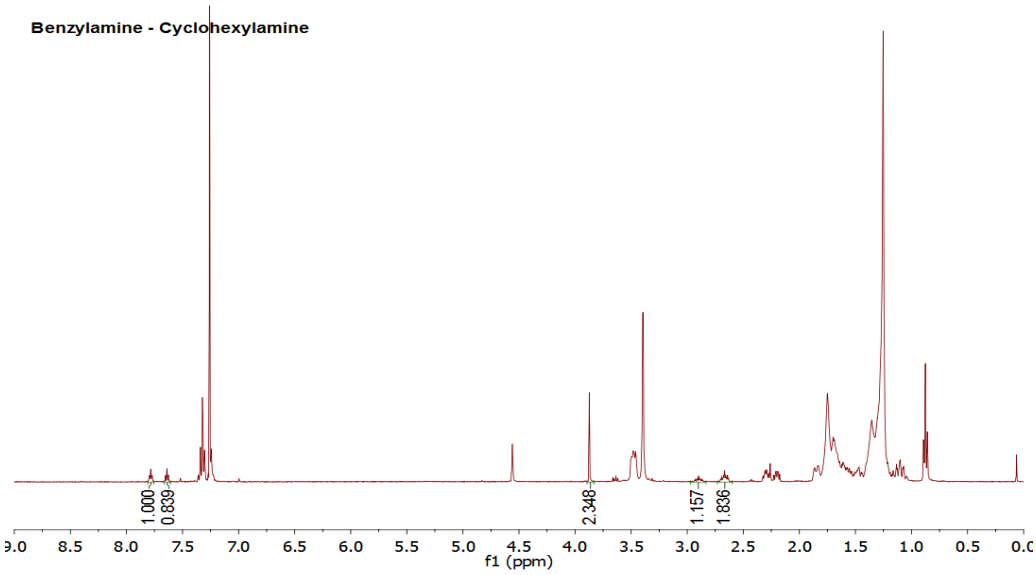
Benzylamine - Cyclohexylamine
1.000
0.839
2.348
1.157
1.836
f1 (ppm)

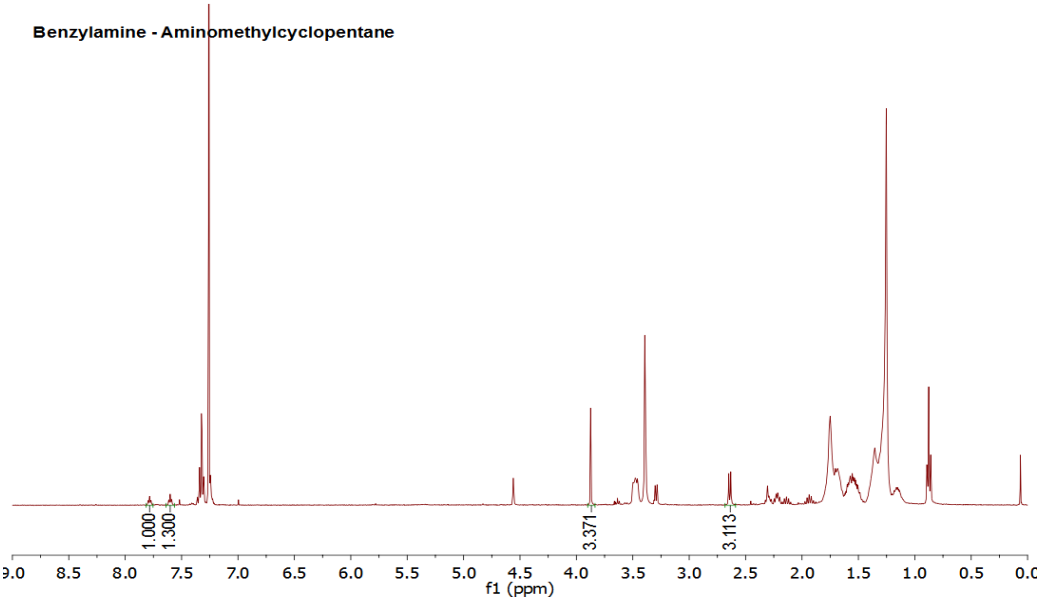
Benzylamine - Aminomethylcyclopentane
1.000
1.300
3.371
3.113
f1 (ppm)

Benzylamine - 1-Pentylamine

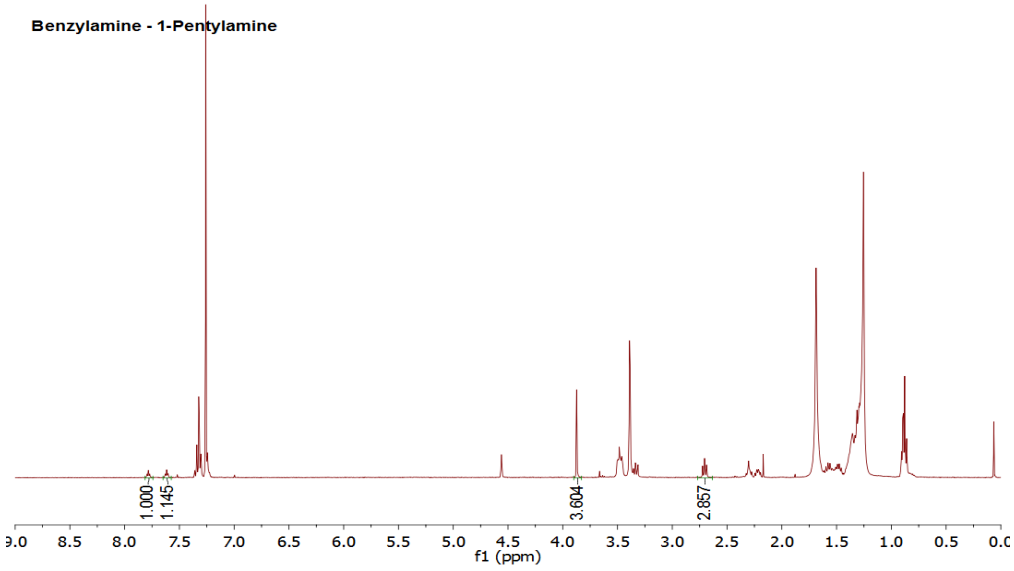

Benzylamine - 3,3-Dimethylbutylamine

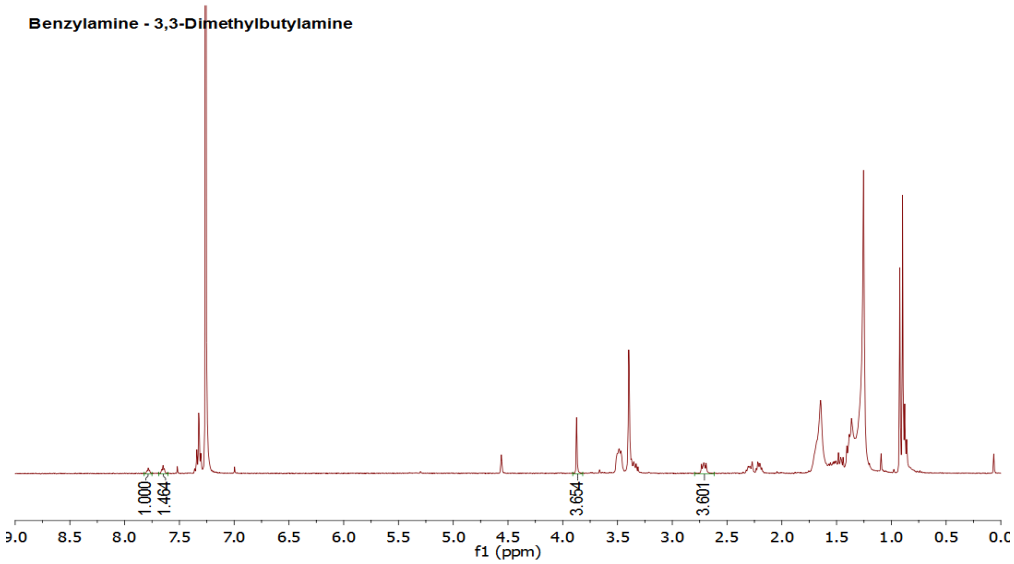

Benzylamine - Hexylamine

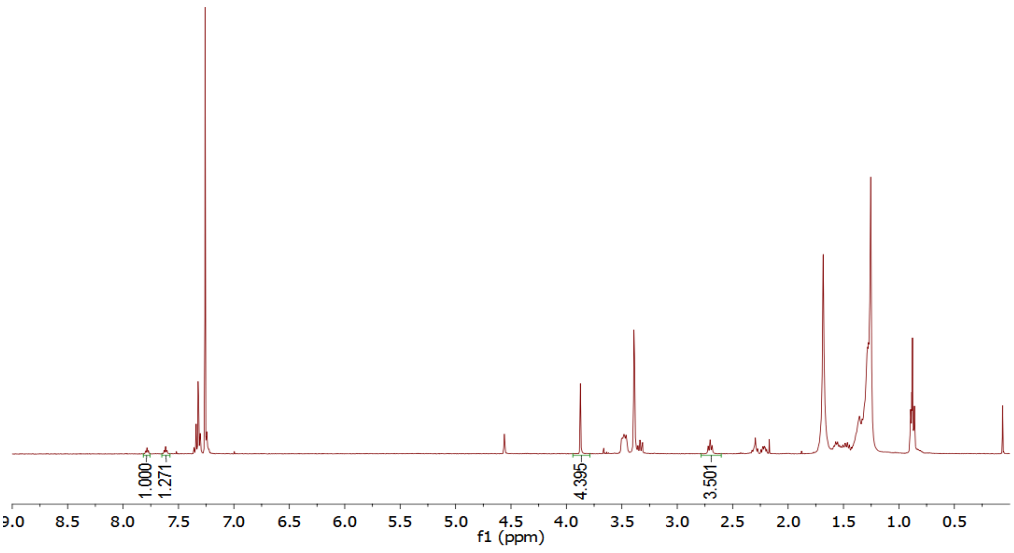

Benzylamine - 1-Naphthylmethylamine

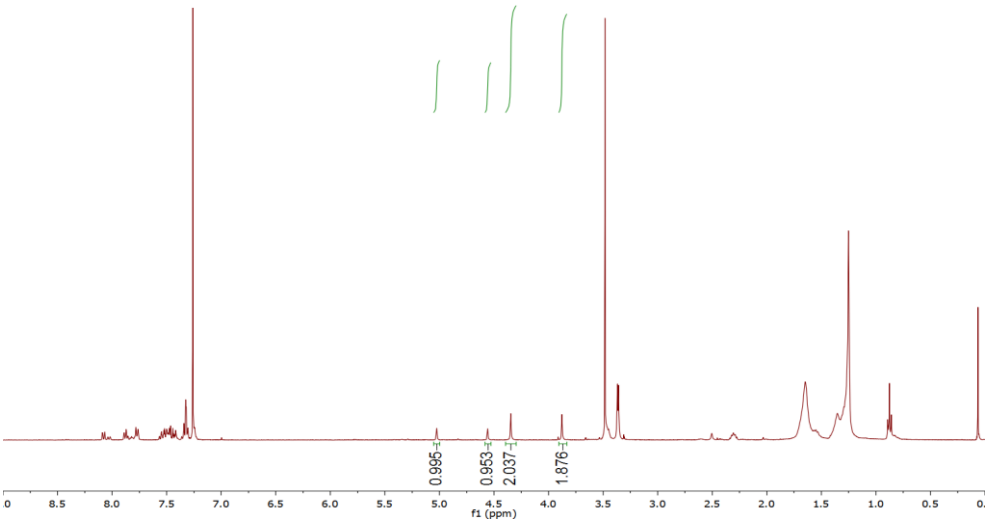

Benzylamine - Heptylamine

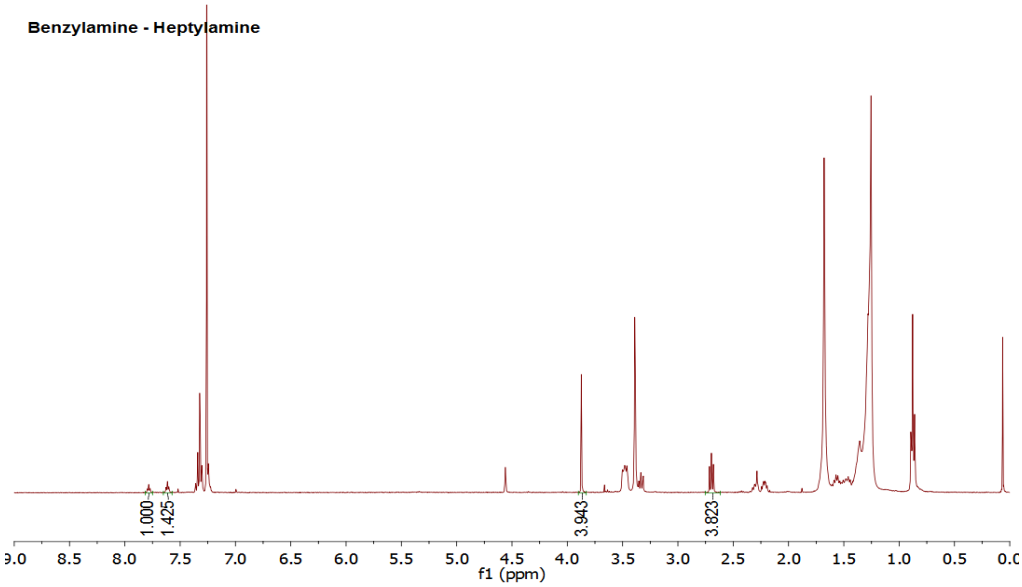

Benzylamine - 1-Octylamine

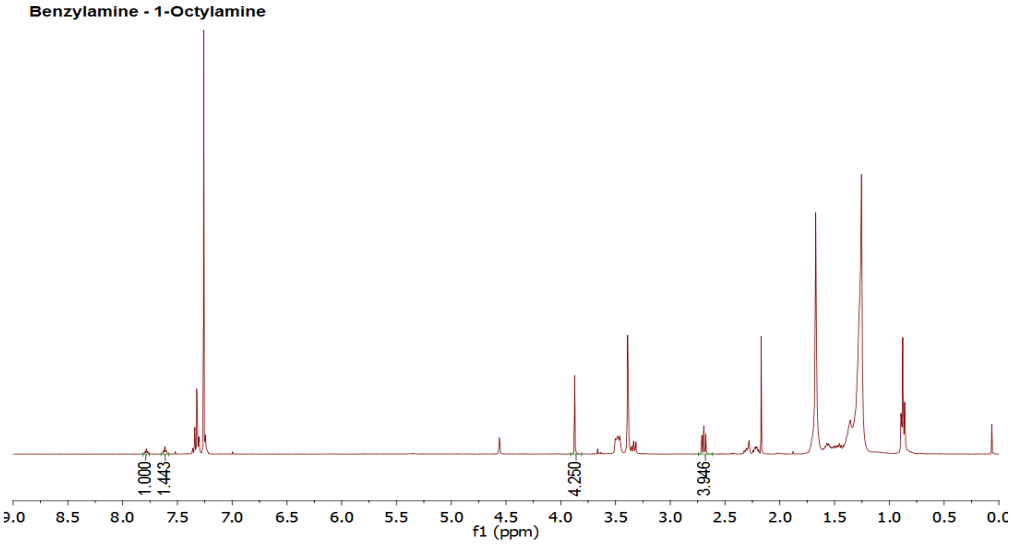

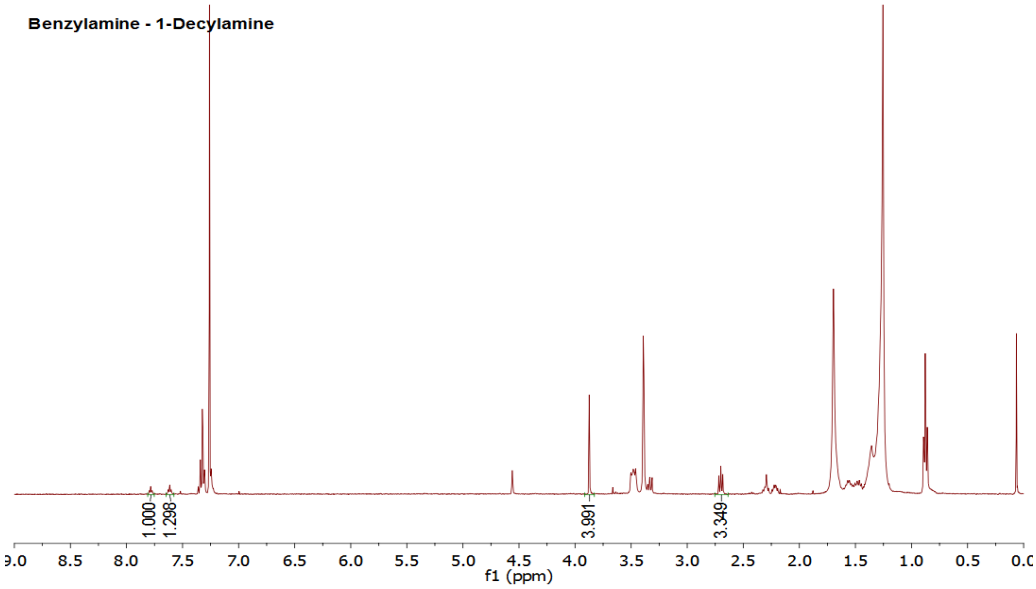

13.4 NMR spectra of exchanging mixtures in D_2O

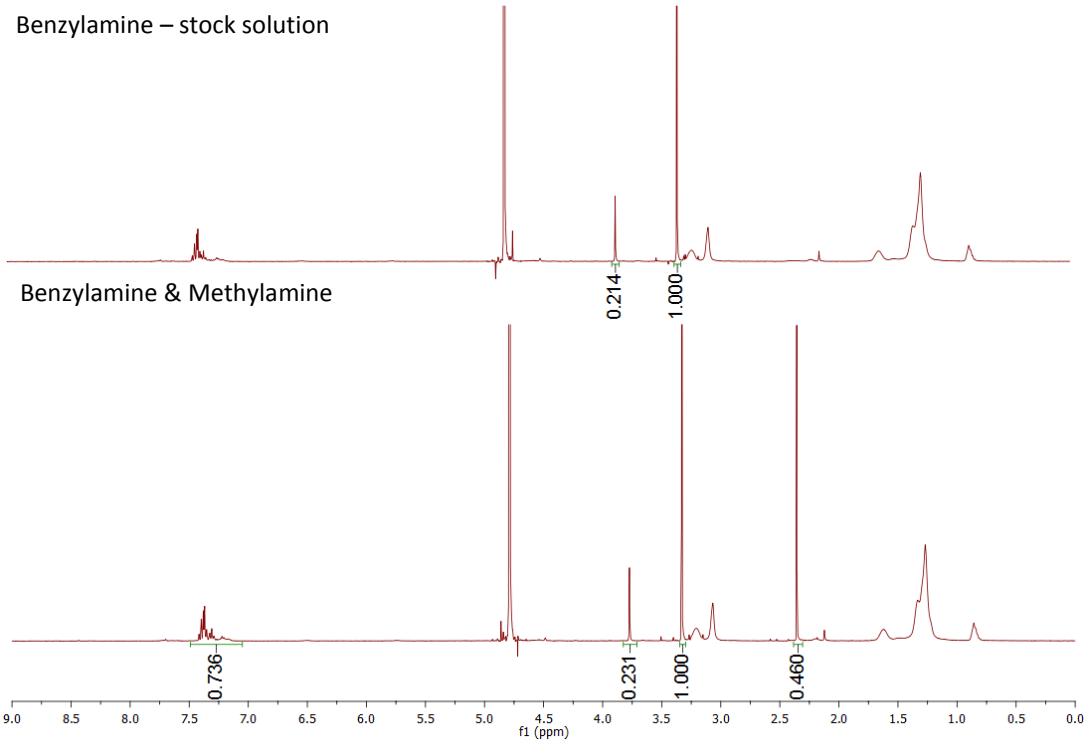

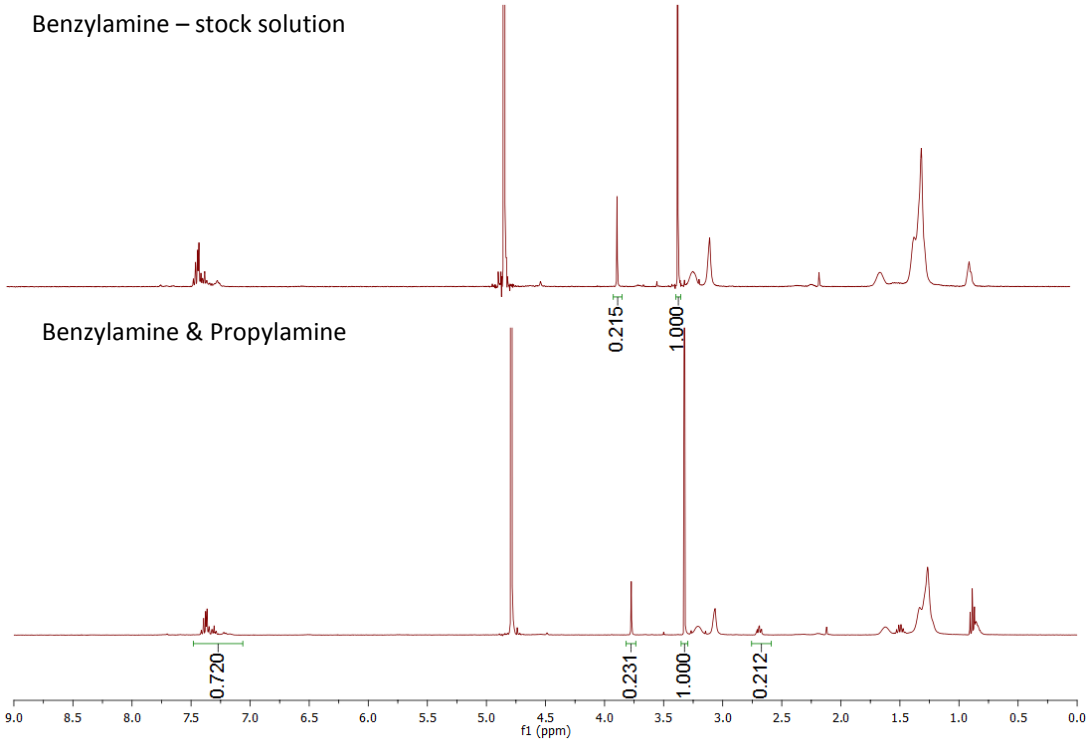
Benzylamine – stock solution
0.215
1.000
Benzylamine & Propylamine
0.720
0.231
1.000
0.212
9.0 8.5 8.0 7.5 7.0 6.5 6.0 5.5 5.0 4.5 4.0 3.5 3.0 2.5 2.0 1.5 1.0 0.5 0.0
f1 (ppm)

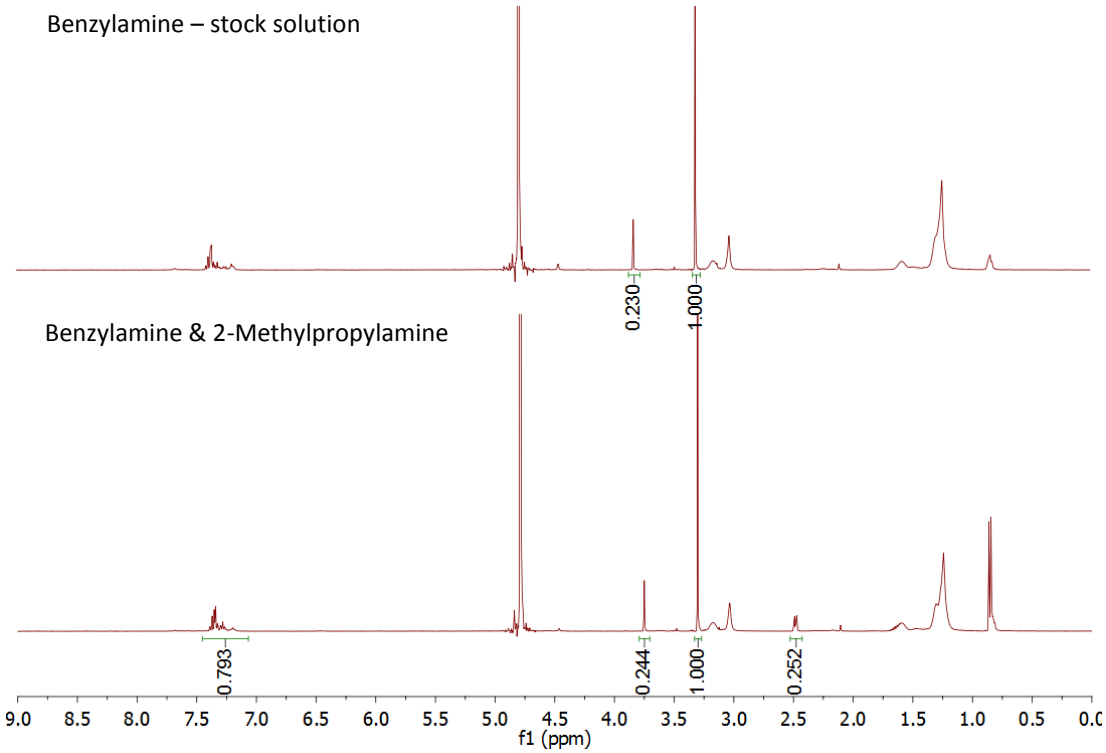
Benzylamine – stock solution
0.230
1.000
Benzylamine & 2-Methylpropylamine
0.793
0.244
1.000
0.252
9.0 8.5 8.0 7.5 7.0 6.5 6.0 5.5 5.0 4.5 4.0 3.5 3.0 2.5 2.0 1.5 1.0 0.5 0.0
f1 (ppm)

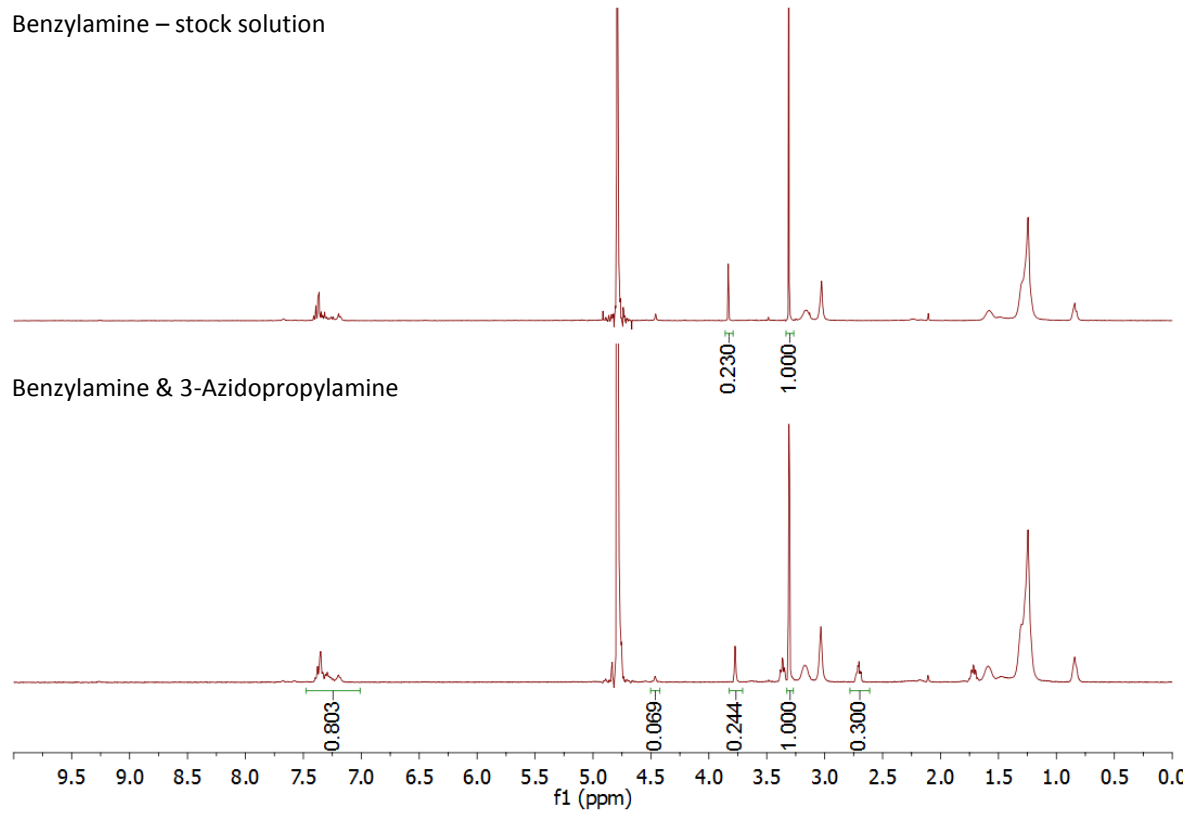
Benzylamine – stock solution
0.230
1.000
Benzylamine & 3-Azidopropylamine
0.803
0.069
0.244
1.000
0.300
9.5 9.0 8.5 8.0 7.5 7.0 6.5 6.0 5.5 5.0 4.5 4.0 3.5 3.0 2.5 2.0 1.5 1.0 0.5 0.0
f1 (ppm)

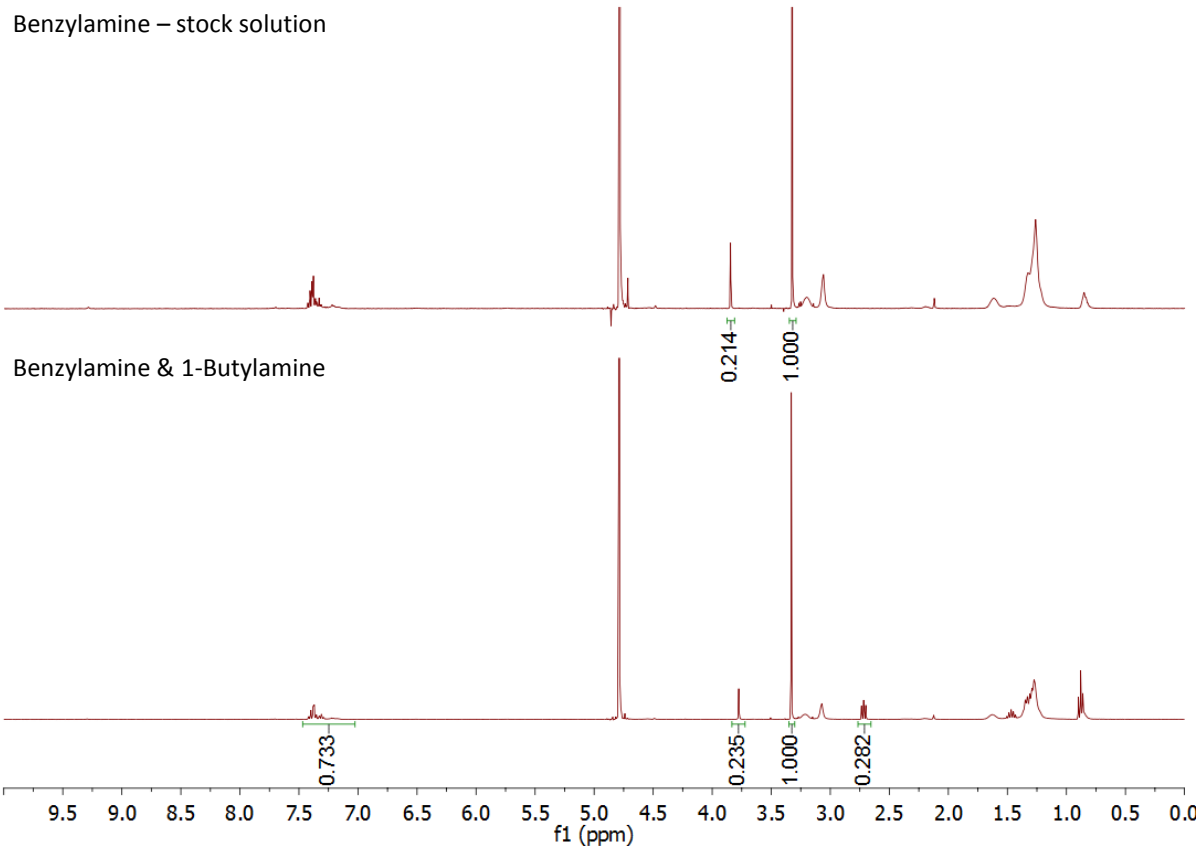
Benzylamine – stock solution
0.214
1.000
Benzylamine & 1-Butylamine
0.733
0.235
1.000
0.282
9.5 9.0 8.5 8.0 7.5 7.0 6.5 6.0 5.5 5.0 4.5 4.0 3.5 3.0 2.5 2.0 1.5 1.0 0.5 0.0
f1 (ppm)

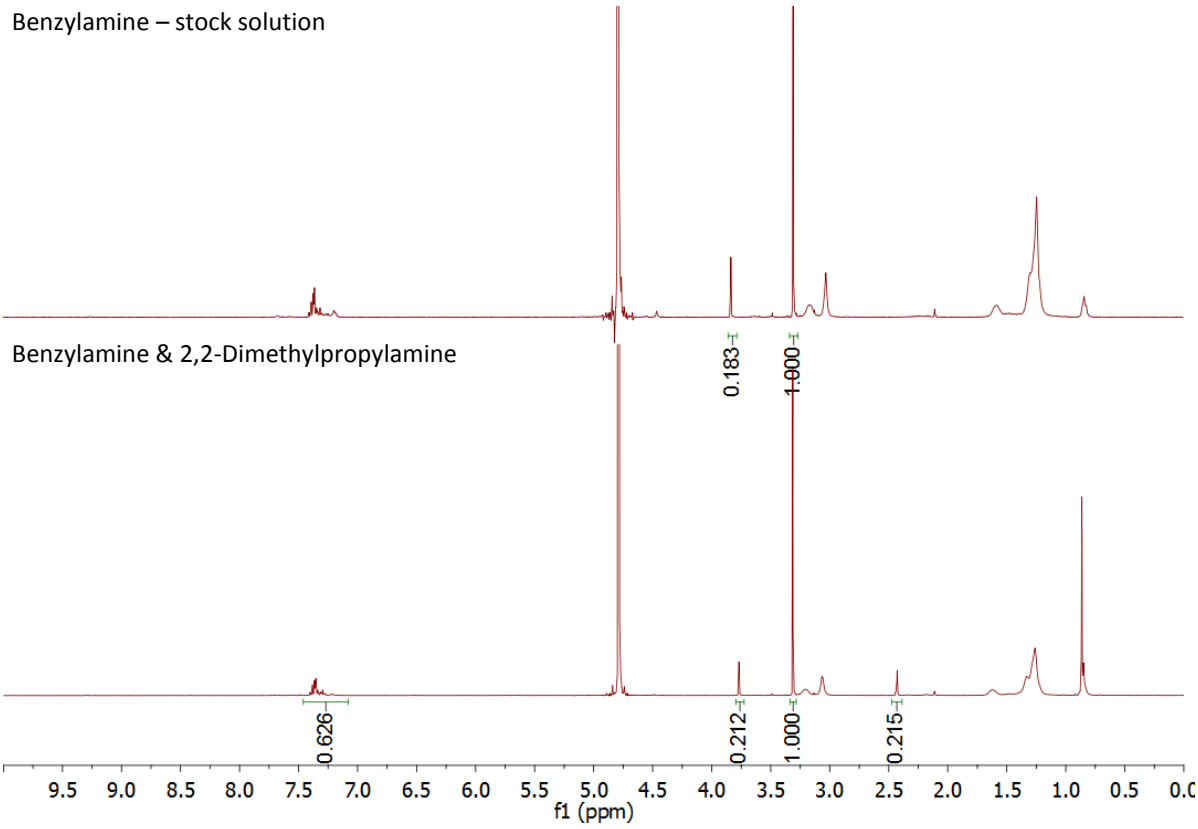
Benzylamine – stock solution
Benzylamine & 2,2-Dimethylpropylamine
0.183
1.000
0.626
0.212
1.000
0.215
9.5 9.0 8.5 8.0 7.5 7.0 6.5 6.0 5.5 5.0 4.5 4.0 3.5 3.0 2.5 2.0 1.5 1.0 0.5 0.0
f1 (ppm)

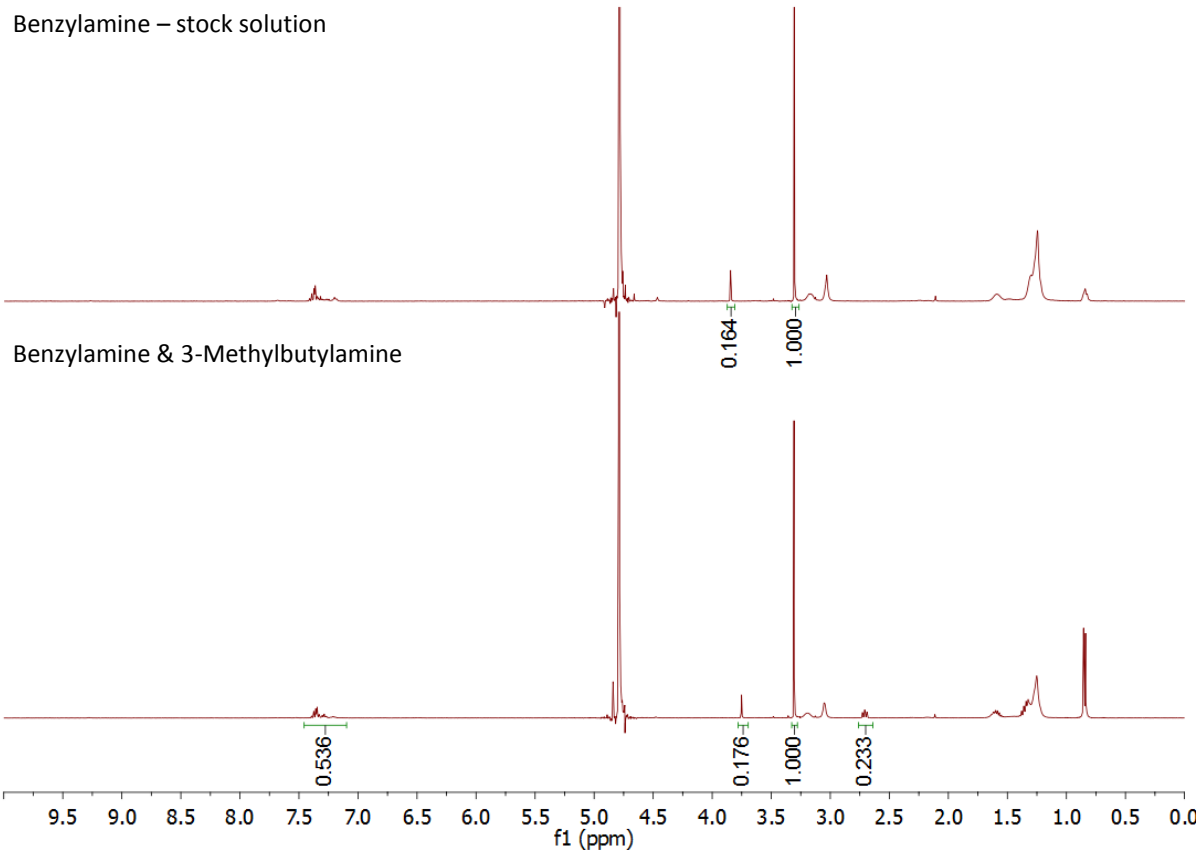
Benzylamine – stock solution
Benzylamine & 3-Methylbutylamine
0.164
1.000
0.536
0.176
1.000
0.233
9.5 9.0 8.5 8.0 7.5 7.0 6.5 6.0 5.5 5.0 4.5 4.0 3.5 3.0 2.5 2.0 1.5 1.0 0.5 0.0
f1 (ppm)

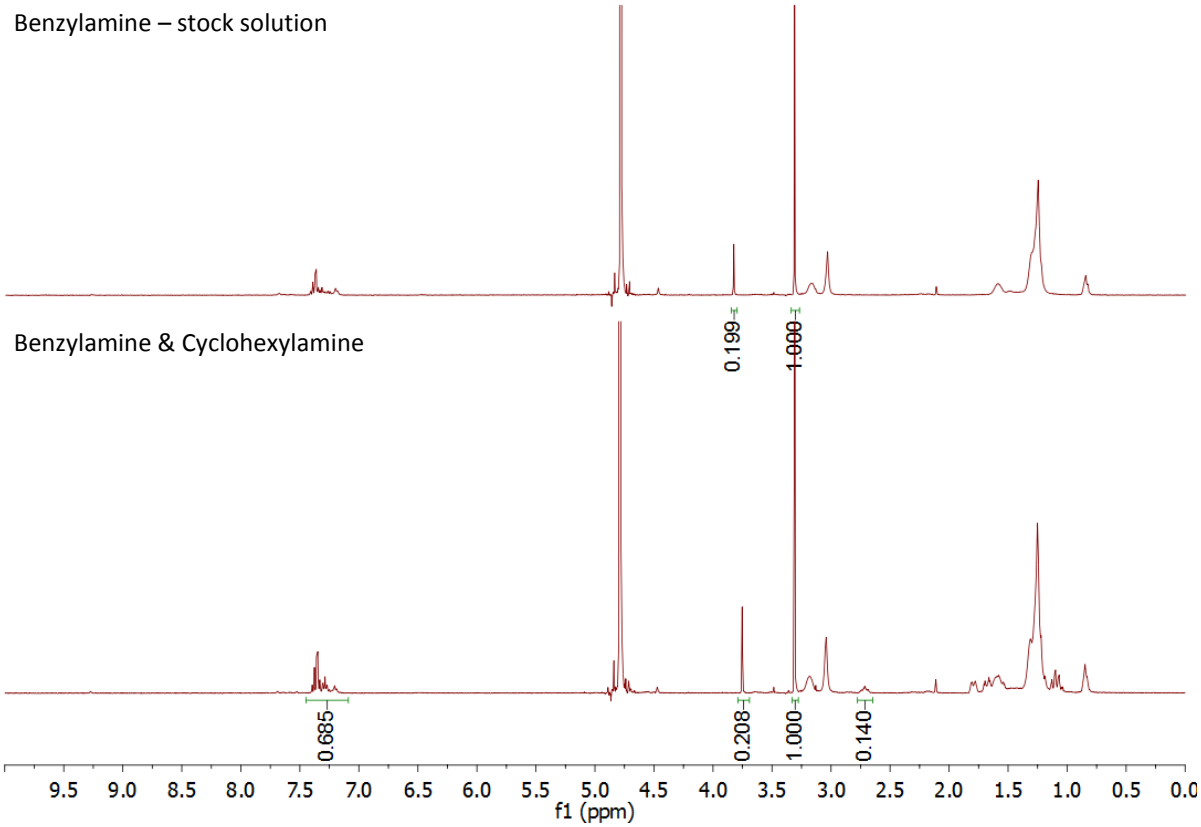
Benzylamine – stock solution
Benzylamine & Cyclohexylamine
0.199
1.000
0.685
0.208
1.000
0.140
9.5 9.0 8.5 8.0 7.5 7.0 6.5 6.0 5.5 5.0 4.5 4.0 3.5 3.0 2.5 2.0 1.5 1.0 0.5 0.0
f1 (ppm)

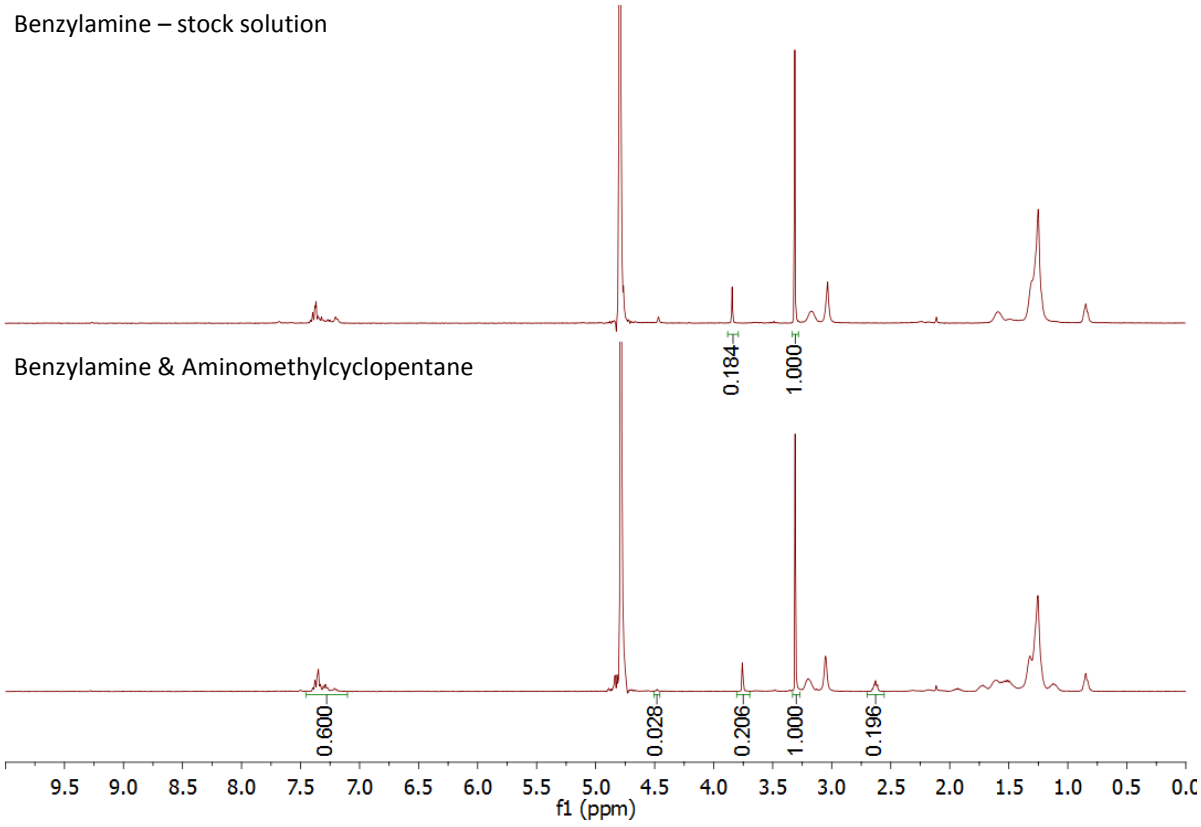
Benzylamine – stock solution
Benzylamine & Aminomethylcyclopentane
0.184
1.000
0.600
0.028
0.206
1.000
0.196
9.5 9.0 8.5 8.0 7.5 7.0 6.5 6.0 5.5 5.0 4.5 4.0 3.5 3.0 2.5 2.0 1.5 1.0 0.5 0.0
f1 (ppm)

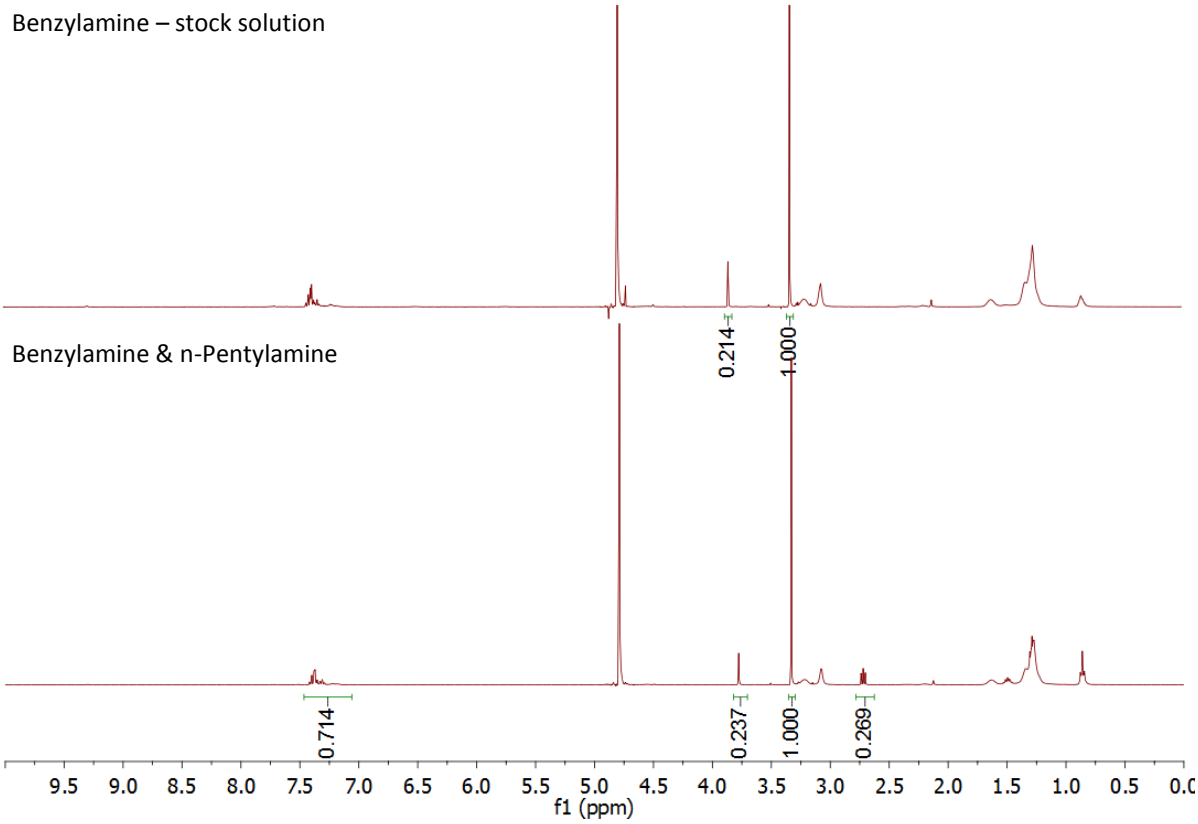
Benzylamine – stock solution
0.214
1.000
Benzylamine & n-Pentylamine
0.714
0.237
1.000
0.269
9.5 9.0 8.5 8.0 7.5 7.0 6.5 6.0 5.5 5.0 4.5 4.0 3.5 3.0 2.5 2.0 1.5 1.0 0.5 0.0
f1 (ppm)

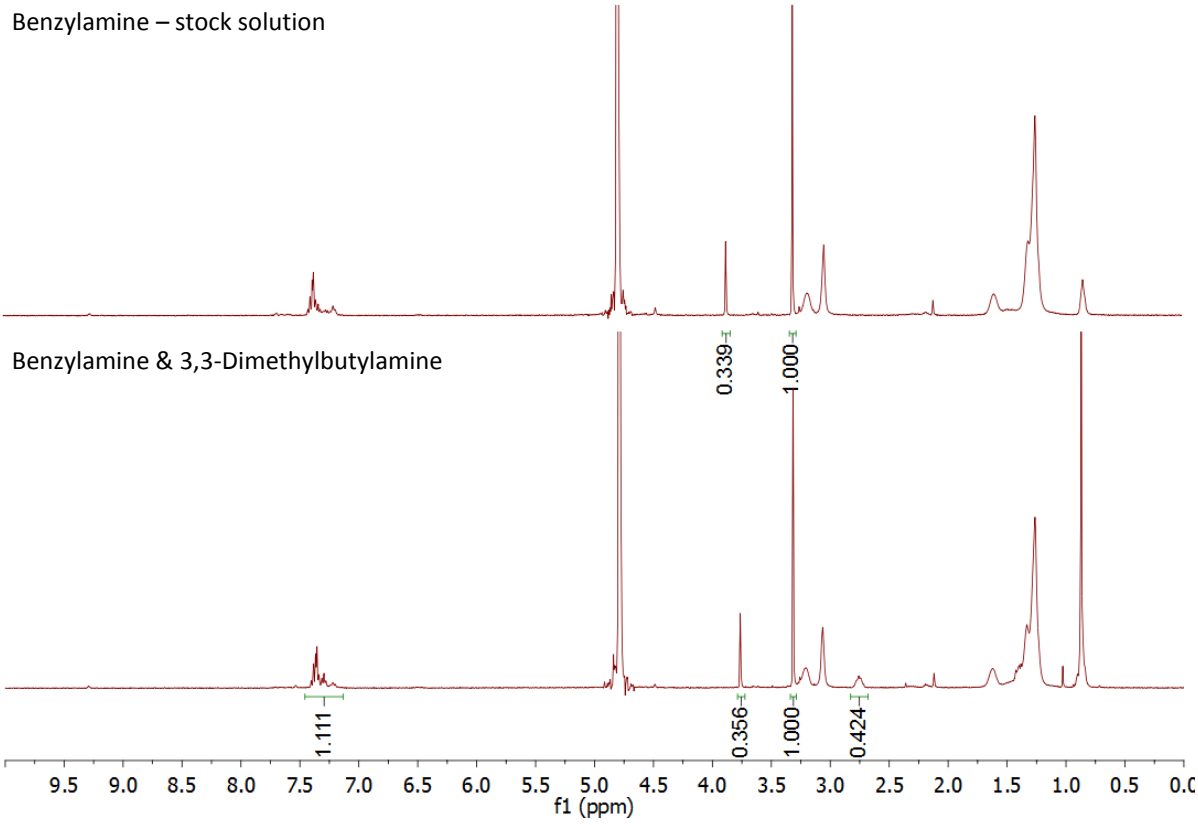
Benzylamine – stock solution
0.339
1.000
Benzylamine & 3,3-Dimethylbutylamine
1.111
0.356
1.000
0.424
9.5 9.0 8.5 8.0 7.5 7.0 6.5 6.0 5.5 5.0 4.5 4.0 3.5 3.0 2.5 2.0 1.5 1.0 0.5 0.0
f1 (ppm)

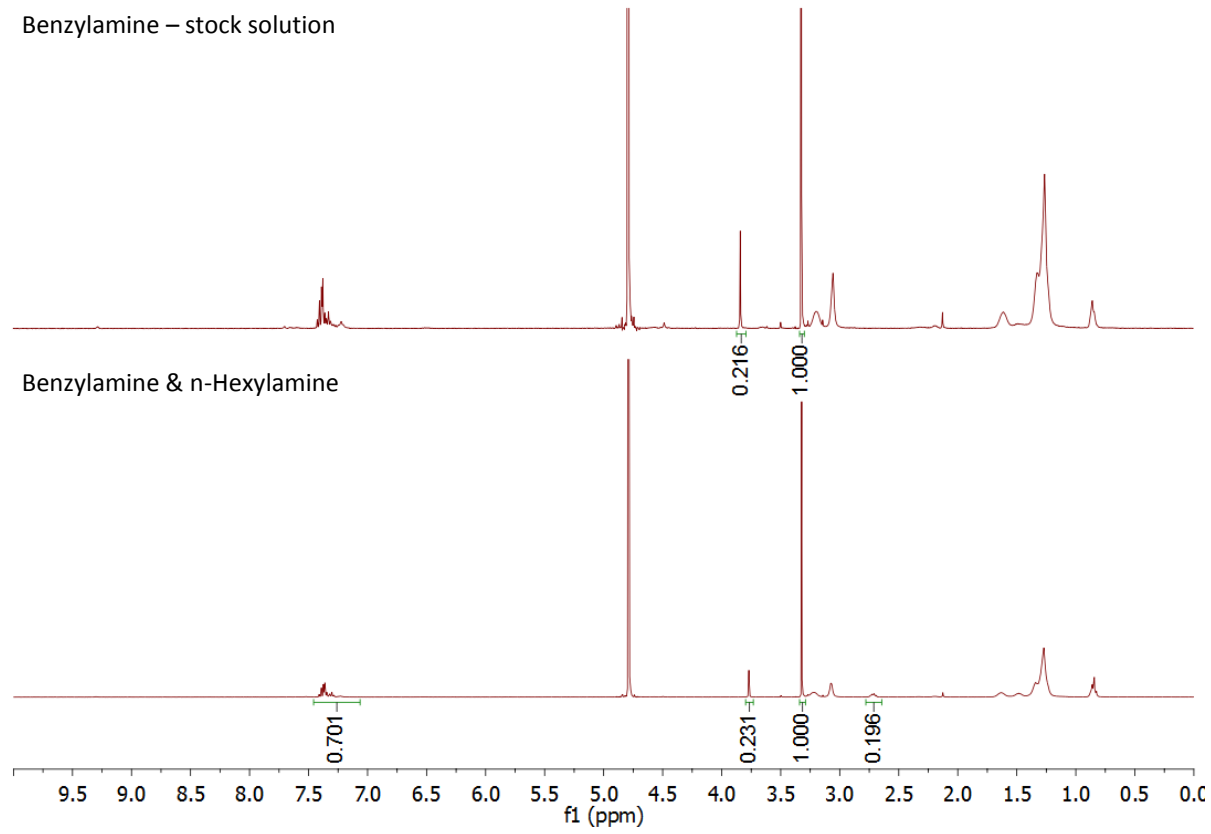
Benzylamine – stock solution
0.216
1.000
Benzylamine & n-Hexylamine
0.701
0.231
1.000
0.196
9.5 9.0 8.5 8.0 7.5 7.0 6.5 6.0 5.5 5.0 4.5 4.0 3.5 3.0 2.5 2.0 1.5 1.0 0.5 0.0
f1 (ppm)

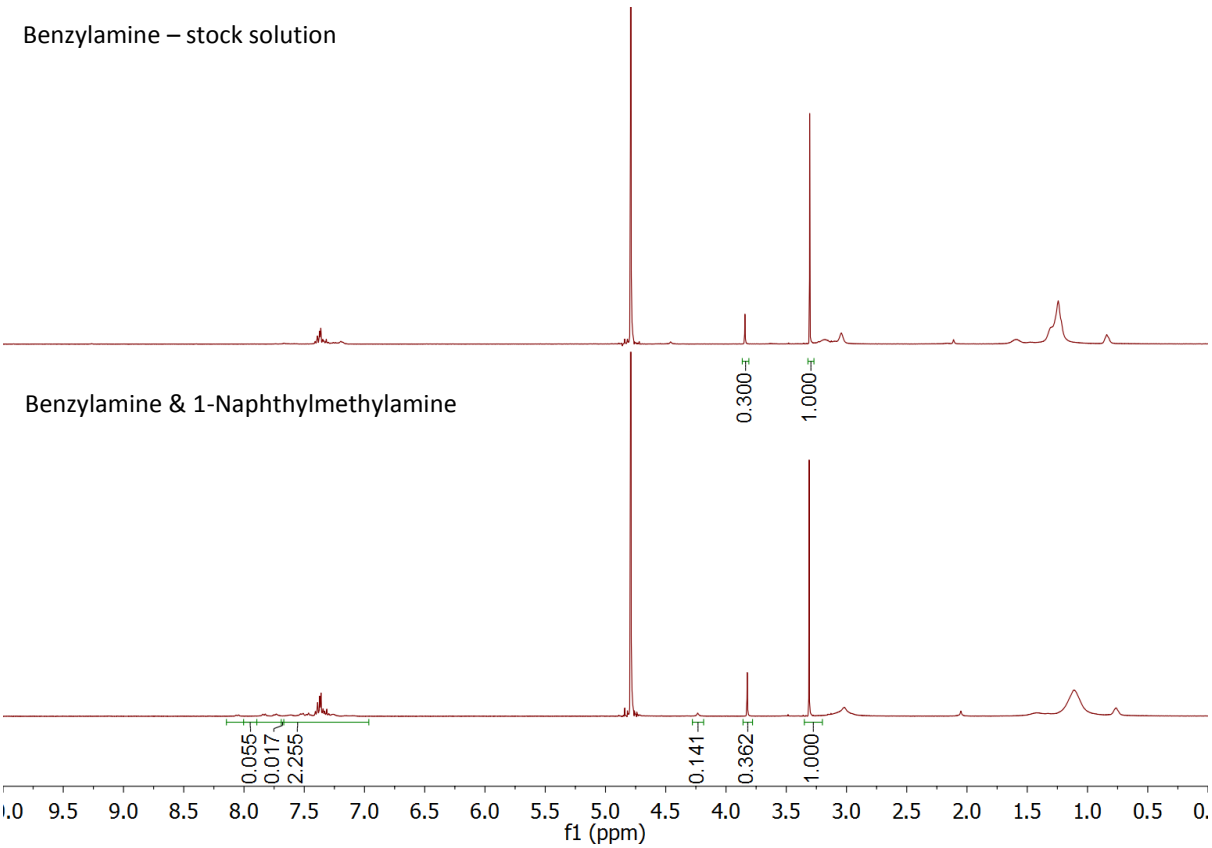
Benzylamine – stock solution
0.300
1.000
Benzylamine & 1-Naphthylmethylamine
0.055
0.017
2.255
0.141
0.362
1.000
9.5 9.0 8.5 8.0 7.5 7.0 6.5 6.0 5.5 5.0 4.5 4.0 3.5 3.0 2.5 2.0 1.5 1.0 0.5
f1 (ppm)

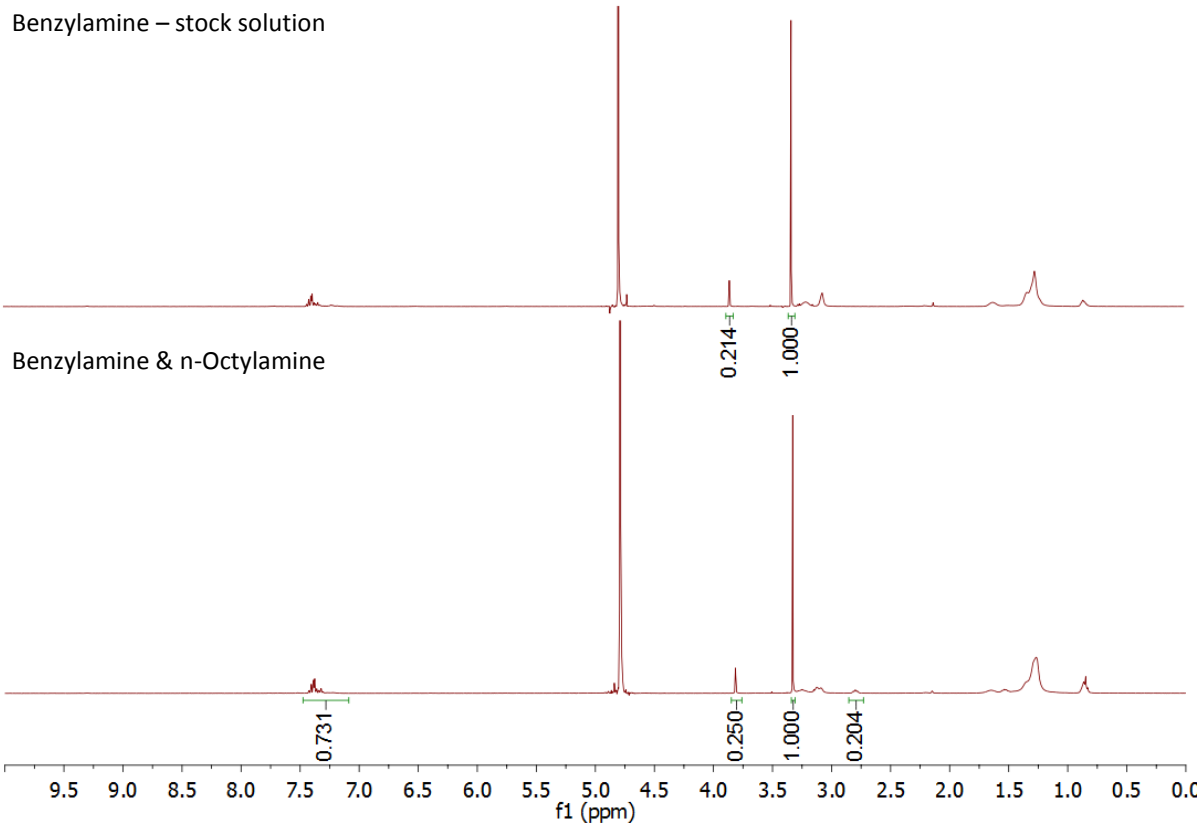
Benzylamine – stock solution
0.214
1.000
Benzylamine & n-Octylamine
0.731
0.250
1.000
0.204
9.5 9.0 8.5 8.0 7.5 7.0 6.5 6.0 5.5 5.0 4.5 4.0 3.5 3.0 2.5 2.0 1.5 1.0 0.5 0.0
f1 (ppm)

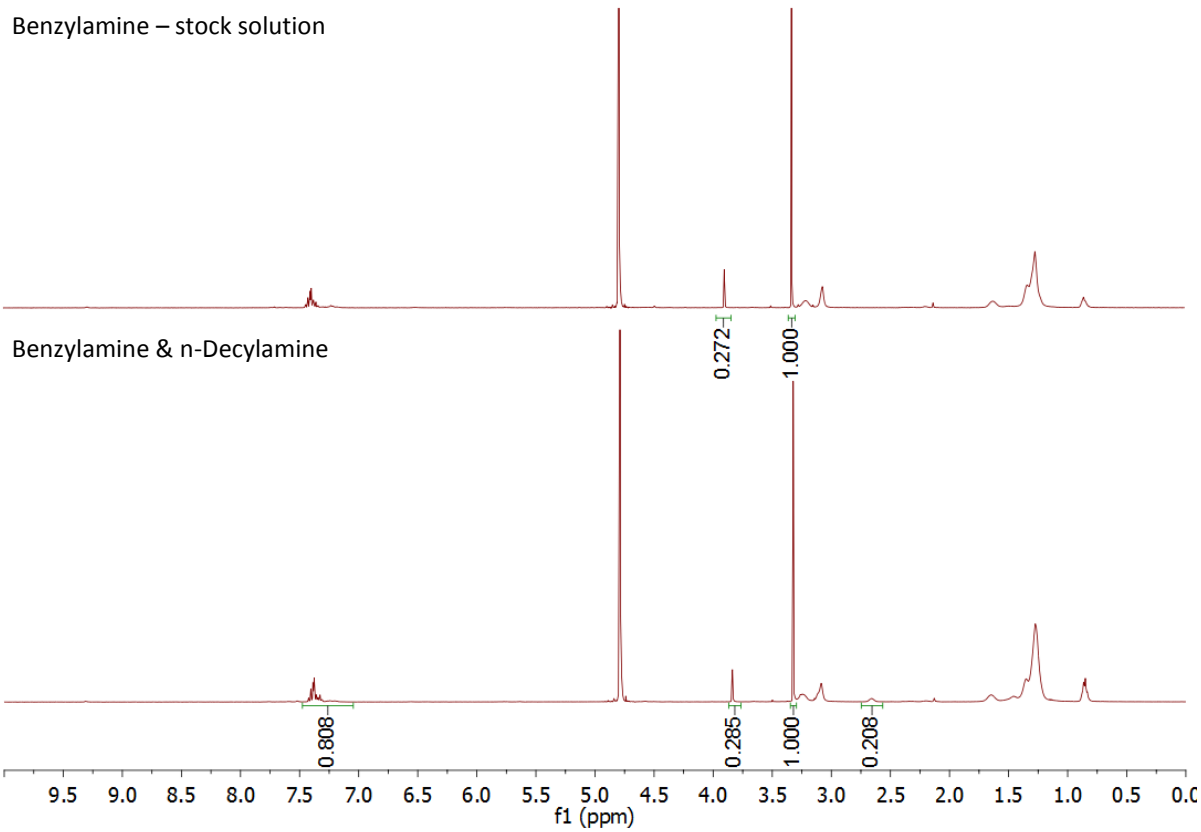
Benzylamine – stock solution
0.272
1.000
Benzylamine & n-Decylamine
0.808
0.285
1.000
0.208
9.5 9.0 8.5 8.0 7.5 7.0 6.5 6.0 5.5 5.0 4.5 4.0 3.5 3.0 2.5 2.0 1.5 1.0 0.5 0.0
f1 (ppm)

14. pH dependence of iminolipid formation and lipid self-assembly

14.1 pH dependence of iminolipid formation

The pH dependence of iminolipid formation from aldehyde lipid **1** and an amine was ascertained using amine **2e** (pK_a = 10.69)[6] as an exemplar. A suspension of vesicles was formed using the standard protocols (10 mL, 4.6 mM **3e** formed by mixing 4.6 mM **1** with 5 eq. **2e**). The pD was measured, giving a value of 12.3, and the ^{1}H NMR spectrum recorded. All experiments were carried out at room temperature, and each NMR sample (0.65 mL) was collected from this 10 mL stock solution. All pD measurements recorded on a Hamilton BioTrode lab pH electrode with HF glass membrane cylindrical and S7 connector (Sigma Aldrich), and converted to pD by adding 0.4.[7] The pD was changed from the initial value of 12.3 to 2.6 by addition of appropriate aliquots of DCl (20 wt% in D_2O). The reverse titration (from pD 2.6 to 11.5) was carried out by adding appropriate aliquots of NaOD (10 wt% in D_2O).

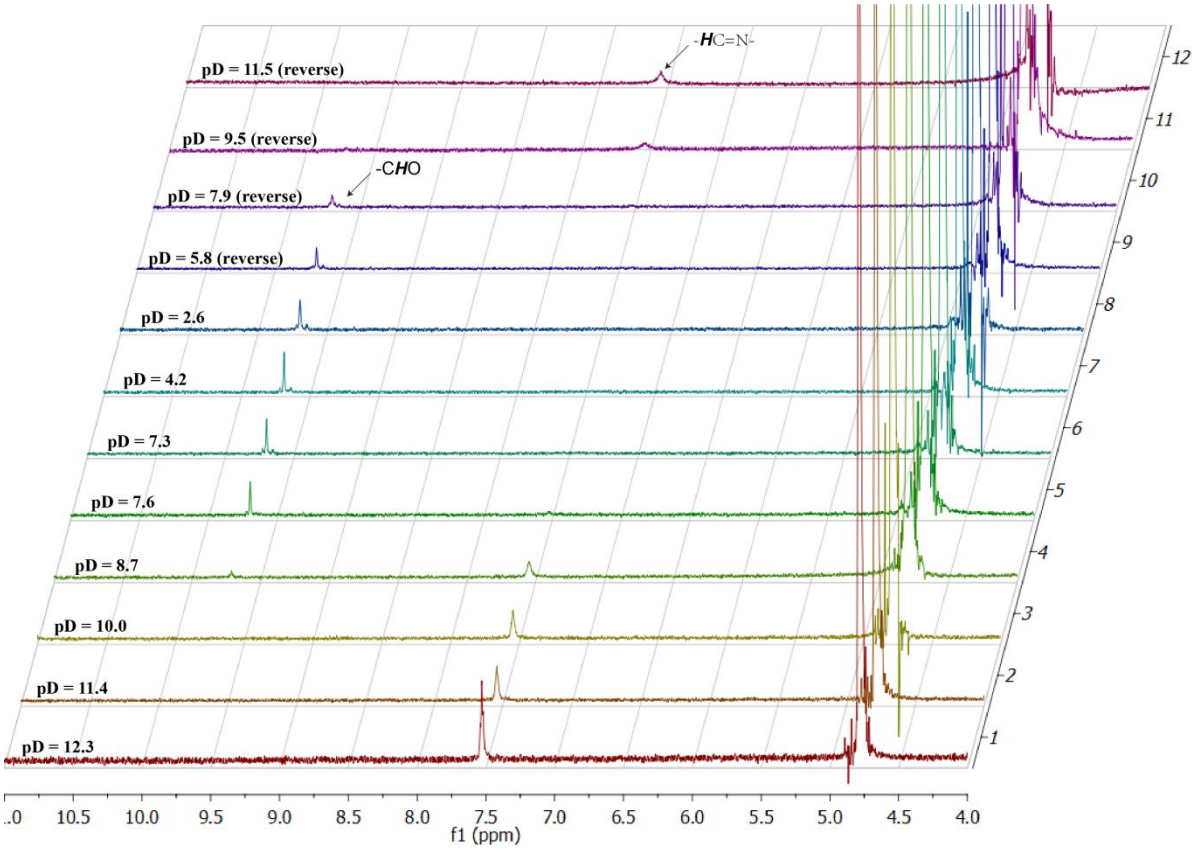

Figure S17. ^{1}H NMR spectra for a 4.6 mM **3e** suspension (10 mL, 4.6 mM **1** with 5 eq. **2e** to give a **3e** suspension in D_2O) as a function of pD.

At pD 8.7, an aldehyde resonance became visible, which became progressively stronger as the pD decreased further, accompanied by the loss of the resonance from the imine CH=N. The conversion of imine **3e** to aldehyde **1** was calculated from the integration of the respective resonances, e.g. at

pD 8.7, approximately 16% of the total lipid was present as the aldehyde (Figure S17). This change was reversible upon the addition of base, with the reappearance of the imine resonance as the solution became more alkaline.

The titration revealed that an equivalence point ([**2e**] = [**3e**]) was reached at pD ~8. A small amount of hysteresis was observed, which could be due to either changes in the iminolipid self-assembly process or the accumulation of salt in solution (Figure S18).

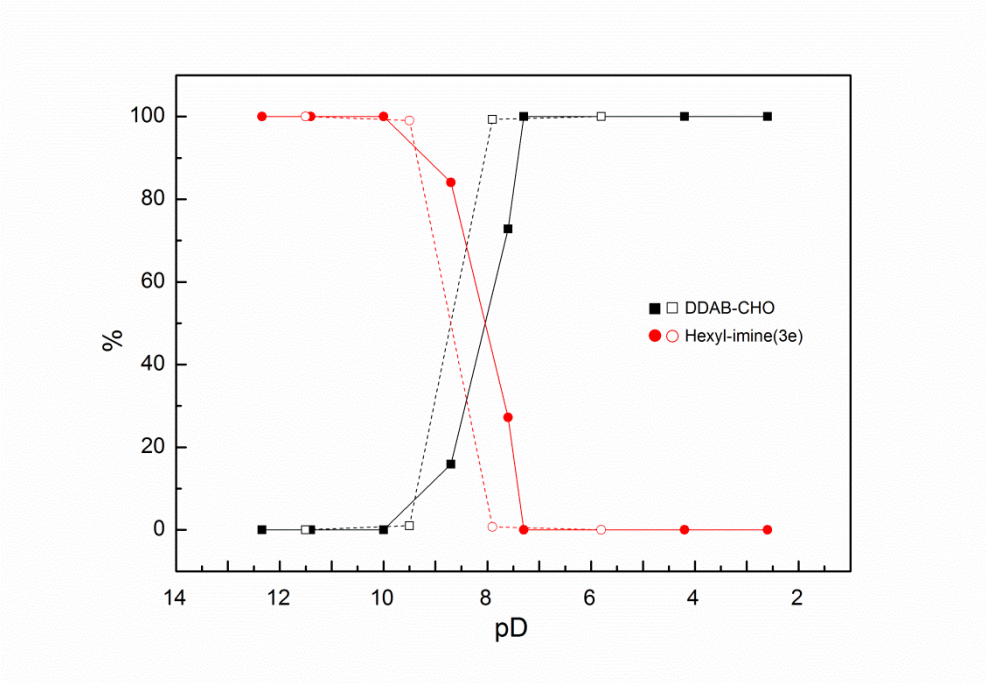

Figure S18: Proportions of DDAB-CHO **1** (squares, black) and imine **3e** (circles, red) for NMR samples collected from stock solution of **3e** (10 mL, 4.6 mM **1** and 5 eq. **2e** to give a **3e** suspension in D_2O at pD 12.3) as a function of pD at room temperature. The filled squares and circles showed a conversion of imine **3e** (●) to aldehyde **1** (■) from pD 10 to 7.3 (complete, 100% aldehyde). The hollow squares and circles showed a reverse process of conversion of aldehyde **1** (□) to imine **3e** (○) from pD 7.9 to 9.5 (complete, 100% imine). pDs were adjusted by DCl (20 wt% in D_2O) or NaOD (10 wt% in D_2O) solution.

14.2 pH dependence of lipid self-assembly

Although the ^{1}H NMR spectra obtained during titration with acid indicated that the iminolipids were largely dissociated below pD 7.5, this titration did not provide information on the self-assembled structures (e.g. bilayer structures) that may be present at these different pH values.

A pH titration of vesicle suspensions of both aldehyde **1** and iminolipid **2e** that were loaded with Nile Red (1 µM) using standard methodology (see ESI Section 7) showed that the emission of Nile Red changed little of the course of the titration (Figure S19), which we ascribe to the self-assembly of

lipid **1** providing hydrophobic environments for the Nile Red even after the hydrolysis of the iminolipid **2e**.

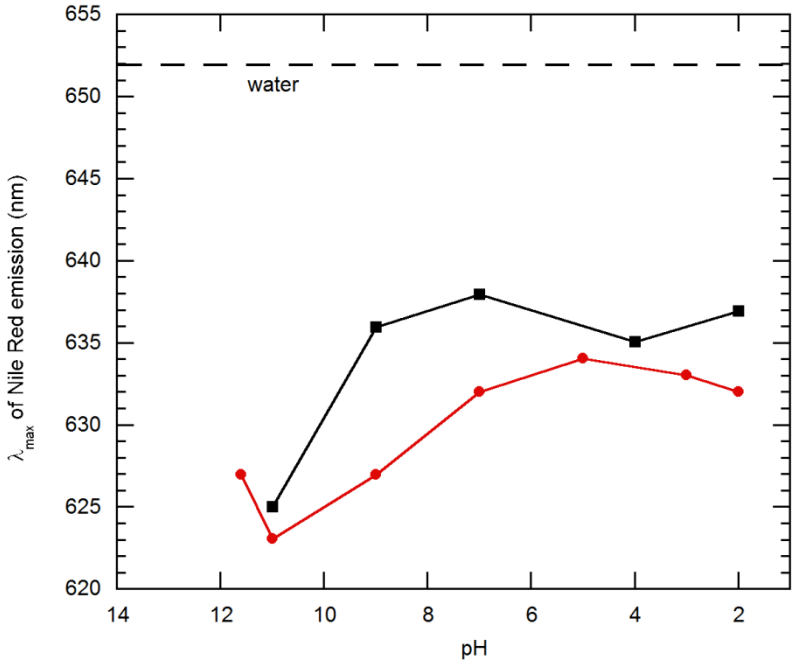

Figure S19: Fluorescence emission maxima from Nile Red in suspensions of aldehyde lipid **1** (4.6 mM) in H_2O (■) and iminolipid **3e** (10 mL, 4.6 mM **1** and 5 eq. **2e** to give a **3e** suspension) in H_2O (●) as a function of pH. Nile Red emission in water is observed at (652 ± 2) nm.

15. The reverse additions used to verify the K_{rel} values obtained in D_2O

To verify that these K_{rel} values indicate the true position of the equilibrium, additional equilibriating mixtures were created using 1-naphthylmethylamine in the reference sample.

For example:

- Hexylamine (**2e**) added to benzyliminolipid (**3p**)

$$K_{rel(1)} = \frac{[hexyl-imine][benzyl-amine]}{[benzyl-imine][hexyl-amine]}$$

- 1-Naphthylmethylamine (**2q**) added to benzyliminolipid (**3p**)

$$K_{rel(2)} = \frac{[naphthylmethyl-imine][benzyl-amine]}{[benzyl-imine][naphthylmethyl-amine]}$$

- *n*-Hexylamine (**2e**) added to 1-naphthylmethyliminolipid (**3q**)

$$K_{rel(3)} = \frac{[hexyl-imine][naphthylmethyl-amine]}{[naphthylmethyl-imine][hexyl-amine]}$$

If all the three mixtures were at equilibrium, then the follow relationship should be satisfied:

$$K_{rel(3)} = \frac{K_{rel(1)}}{K_{rel(2)}}$$

The K_{rel} value for exchange of the amine of interest with benzyliminolipid (**3p**) can be found in **Table S2**. The amines selected for this verification were methylamine (**2a**), aminomethylcyclopentane (**2m**) and hexylamine (**2e**).

For reference samples containing **3q**, methanol (0.4 µL in 0.7 mL D_2O, 14.13 mM) was added into each NMR sample as an internal standard as well, as used when benzyliminolipid **3p** was the reference sample. Before the amine of interest was added, the initial amount of free 1-naphthylmethylamine (**2q**) [naphthyl-CH_2NH_2]$_i$ was measured from the relative integration of the methylene resonance (compared to the methanol standard). Any increase in the value of this integral after addition of a different amine (RNH_2) would be ascribable to displacement of 1-naphthylmethylamine from the naphthyliminolipid.

Since both 1-naphthylmethylamine and the naphthyliminolipid have seven naphthyl protons, the integral from 8.2-7.2 ppm (which ***includes*** the very weak imine N=CH resonances from [RN=CH-DDAB]$_f$ and [naphthyl-CH_2N=CH-DDAB]$_f$ at ~7.5 ppm) will give the combined relative concentrations. The final concentration of free 1-naphthylmethylamine [naphthyl-CH_2NH_2]$_f$ can be calculated from

the relative integration of the resonance due to the two methylene protons and the final concentration of free 1-naphthylmethylamine [naphthyl-CH_2NH_2]$_f$ can be calculated from Eqn. (7) below. Therefore the final concentration of the naphthyliminolipid [naphthyl-CH_2N=CH-DDAB]$_f$ can be calculated by subtracting these values from the integral of the aromatic moieties.

The relative concentration of the added amine [RNH_2] can be obtained directly from the ^{1}H NMR spectrum, but the relative concentration of the product iminolipid [RN=CH-DDAB] can only be inferred by the increase in the integral of free benzylamine after addition of RNH_2 due to displacement of 1-naphthylmethylamine from the naphthyliminolipid. Therefore,

$$[RN{=}CH\text{-}DDAB]_f = [naphthyl\text{-}CH_2NH_2]_f - [naphthyl\text{-}CH_2NH_2]_i \quad \textbf{(7)}$$

Combining these values then gives the equilibrium constant K_{rel}.

This can be exemplified with the integrals from the spectra recorded for the addition of *n*-hexylamine to a 1-naphthylmethylamine/lipid **1** mixture.

Integral for CH_2-N of [Naphthyl-CH_2NH_2]$_i$ before *n*-hexylamine (Fig. S17) = 0.108

Integral for CH_2-N of [Naphthyl-CH_2NH_2]$_f$ after *n*-hexylamine (Fig. S18) = 0.155

Integral for CH_2-N of [$CH_3(CH_2)_5NH_2$] after *n*-hexylamine (Fig. S18) = 0.220

Integral for ArH for [Naphthyl-CH_2NH_2]$_f$ + [Naphthyl-CH_2N=CH-DDAB], one proton for the imine N-CH [naphthyl-CH_2N=C**H**-DDAB] and one proton for the imine N-CH [RN=C**H**-DDAB] after *n*-hexylamine (Fig. S18) = 0.982

Therefore:

$$K_{rel} = \frac{K_2}{K_1} = \frac{[RN{=}CH{-}DDAB][NaphthylCH_2NH_2]}{[NaphthylCH_2N{=}CH{-}DDAB][RNH_2]}$$

$$= \frac{\left(\frac{0.155}{2} - \frac{0.108}{2}\right) \times \left(\frac{0.155}{2}\right)}{\left(\frac{0.982 - \frac{0.155}{2} * 7 - \left(\frac{0.155 - 0.108}{2}\right)}{8}\right) \times \left(\frac{0.220}{2}\right)} = 0.32$$

The same method was applied to the other two amines (three samples in each case) to give the values in **Table S3**.

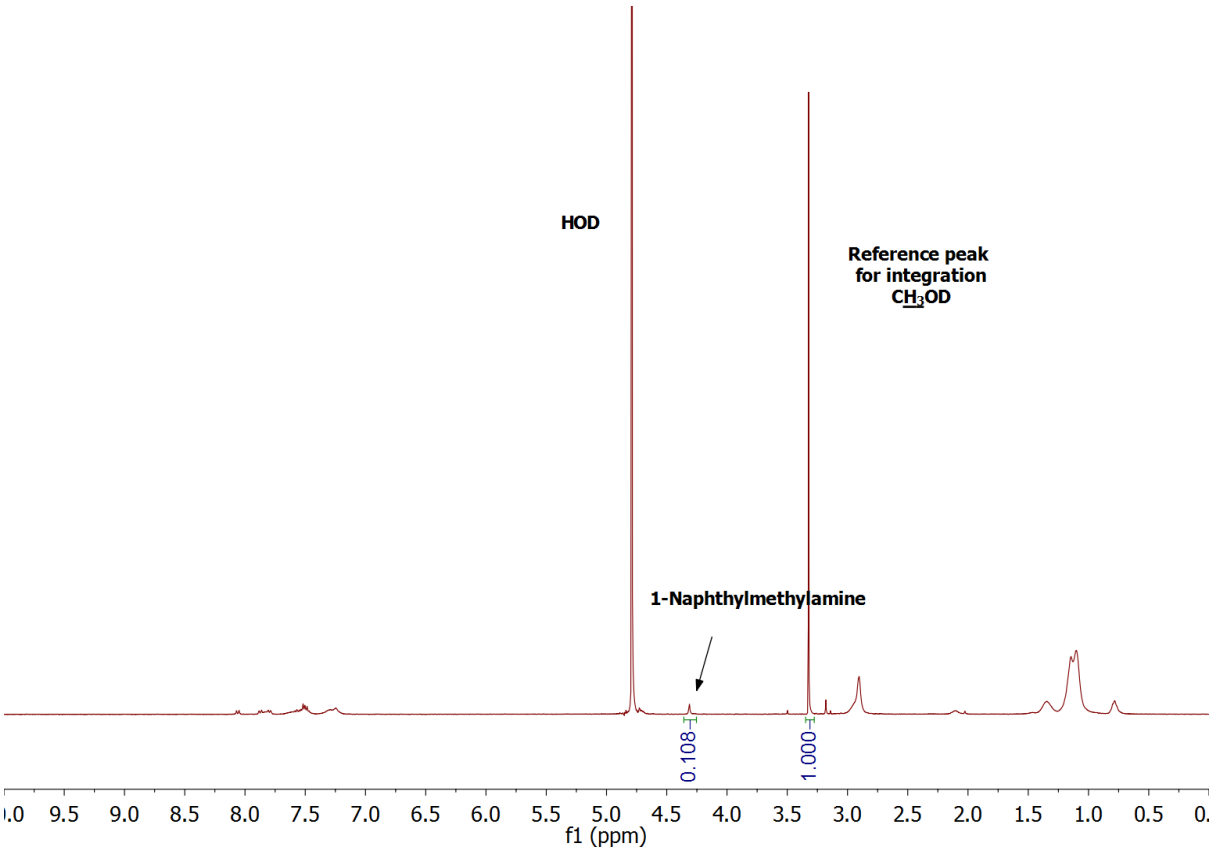

Figure S20. ^{1}H NMR spectrum of naphthylmethylamine with lipid **1** in D_2O.

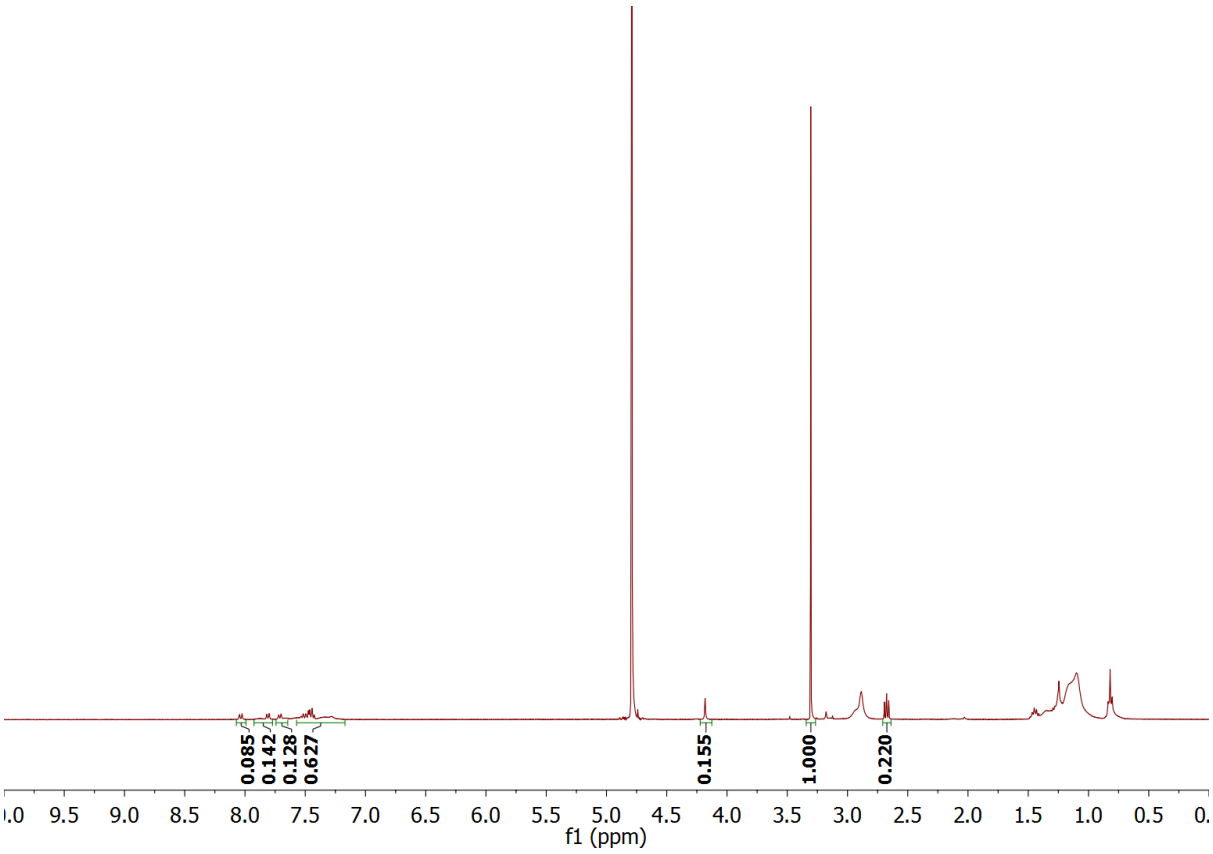

Figure S21. ^{1}H NMR spectrum of 1-naphthylmethylamine with lipid **1** in D_2O after addition of *n*-hexylamine.

Table S3. The relative exchange constant of amines in D_2O based on 1-naphthylamine.

Amine	K_{rel} in D_2O	clogP
Methylamine	0.15 ± 0.15	-0.664
Aminomethylcyclopentane	0.15 ± 0.15	1.427
n-Hexylamine	0.45 ± 0.15	1.981
1-Naphthylmethylamine	1.00	2.268

The data in **Table S2** can now be validated against **Table S3**. For example:

(1) Methylamine (**2a**) to benzyliminolipid (**3p**) $K_{rel(1)}$ = 0.13 ± 0.13

1-Naphthylmethylamine (**2q**) to benzyliminolipid (**3p**) $K_{rel(2)}$ = 2 ± 1

Methylamine (**2a**) to 1-naphthylmethyliminolipid (**3q**) $K_{rel(3)}$ = 0.15 ± 0.15

$$K_{rel(1)} / K_{rel(2)} = \frac{0.13 \pm 0.13}{2 \pm 1} = 0.07 \pm 0.08$$ compared to $K_{rel(3)}$ = 0.15 ± 0.15

(2) Aminomethylcyclopentane (**2m**) to benzyliminolipid (**3p**) $K_{rel(1)}$ = 0.75 ± 0.25

1-Naphthylmethylamine (**2q**) to benzyliminolipid (**3p**) $K_{rel(2)}$ = 2 ± 1

Aminomethylcyclopentane (**2m**) to 1-naphthylmethyliminolipid (**3q**) $K_{rel(3)}$ = 0.15 ± 0.15

$$K_{rel(1)} / K_{rel(2)} = \frac{0.75 \pm 0.25}{2 \pm 1} = 0.375 \pm 0.225$$ compared to $K_{rel(3)}$ = 0.15 ± 0.15

(3) Hexylamine (**2e**) to benzyliminolipid (**3p**) $K_{rel(1)}$ = 1.25 ± 0.25

1-Naphthylmethylamine (**2q**) to benzyliminolipid (**3p**) $K_{rel(2)}$ = 2 ± 1

Hexylamine (**2e**) to 1-naphthylmethyliminolipid (**3q**) $K_{rel(3)}$ = 0.45 ± 0.15

$$K_{rel(1)} / K_{rel(2)} = \frac{1.25 \pm 0.25}{2 \pm 1} = 0.68 \pm 0.37$$ compared to $K_{rel(3)}$ = 0.45 ± 0.15

16. Exfoliation and characterization of layered materials

The surfactants used for exfoliation (5 mg, one of either DDAB, iminolipid **3r** or iminolipid **3s**) were added to a 14 mL glass vial containing graphite (30 mg, 99.5 % grade, purchased from Graphexel) and deionised water (10 mL, conductivity of 18.2 MΩ·cm). The mixture was placed in a bath sonicator (Hilsonic 600 W) for 72 h before centrifugation (Sigma 1-14k) at 3500 rpm for 20 minutes and collection of the supernatant. The graphene concentration of resulting dispersions was determined by UV-visible spectroscopy (Cary 5000) using an extinction coefficient measured at 660

nm of 2460 L g^{-1} m^{-1}.[8] For AFM analysis, the dispersions were dropcast onto a 1 x 1 cm Si/SiO_2 wafer and dried under vacuum at 50 °C. AFM was conducted using a Bruker Multimode 8, scanning over 20 x 20 µm areas with 2048 points. The h-BN dispersions were produced using the same protocol, by replacing graphite with bulk h-BN powder (30 mg, 98 % grade, purchased from Sigma Aldrich). The concentration of h-BN was determined using an extinction coefficient of 1000 L g^{-1} m^{-1}.[9]

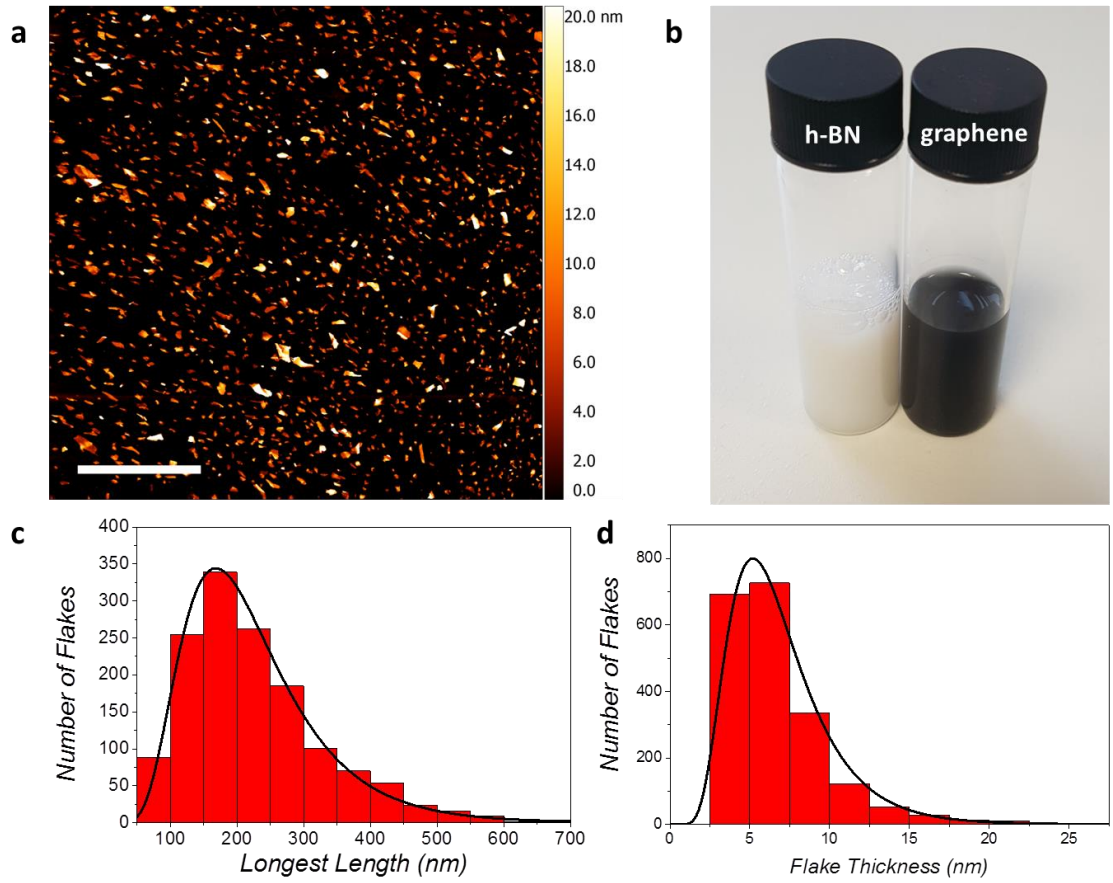

Figure S22. a, 20 x 20 µm scan of graphene flakes dropcast on a silicon substrate (scale bar is 5 µm). **b,** h-BN (left) and graphene (right) dispersions produced using iminolipid **3s** as the exfoliating agent. **c,** Length distribution and **d,** thickness distribution of flakes measured from AFM.

17. References

1. N. A. Porter, H. Vincent, T. Chang, D. R. Magnin and B. T. Wright, *J. Am. Chem. Soc.* 1988, **110**, 3554-3560.

2. F. Hiromichi, Y. Kenzo, H. Tomohoto, K. Ozora, O. Takashi, S. Yoshinari, O. Takuya, M. Tomohiro and K. Yasuyuki, *Chem. Asian J.* 2012, **7**, 367-373.

3. (a) C. B. Minkenberg, W. E.Hendriksen, F. Li, E. Mendes, R. Eelkema and J. H. van Esch, *Chem. Commun.* 2012, **48**, 9837-9839; (b) C. B. Minkenberg, F. Li, P. van Rijn, L. Florusse, J. Boekhoven, M. C. A. Stuart, G. J. M. Koper, R. Eelkema and J. H. van Esch, *Angew. Chem. Int. Ed*. 2011, **50**, 3421-3424; (c) F. R. Alves, M. E. D. Zaniquelli, W. Loh, E. M. S. Castanheira, M. E. C. D. Real Oliveira and E. Feitosa, *J. Colloid Interface Sci.* 2007, **316**, 132-139.

4. J. Pereira-Lachataignerais, R. Pons, P. Panizza, L. Courbin, J. Rouch and O. López, *Chem. Phys. Lipids* 2006, **140**, 88-97.

5. (a) E. Feitosa, R. D. Adati and F. R. Alves, *Colloid. Surface. A.* 2015, **480**, 253-259; (b) E. Feitosa, F. Rosa Alves, A. Niemiec, M. E. C. D. Real Oliveira, E. M. S. Castanheira and A. L. F. Baptista, *Langmuir* 2006, **22**, 3579-3585; (c) E. F. Marques, A. Khan and B. Lindman, *Thermochim. Acta.* 2002, **394**, 31-37; (d) E. Feitosa, J. Jansson and B. Lindman, *Chem. Phys. Lipids* 2006, **142**, 128-132.

6. W. Edwards and D. K. Smith, *J. Am. Chem. Soc*. 2013, **135**, 5911−5920

7. P. K. Glasoe and F. A. Long, *J. Phys. Chem*. 1960, **64**, 188-190

8. Y. Hernandez, V. Nicolosi, M. Lotya, F. M. Blighe, Z. Sun, S. De, I. T. McGovern, B. Holland, M. Byrne, Y. K. Gun'Ko, J. J. Boland, P. Niraj, G. Duesberg, S. Krishnamurthy, R. Goodhue, J. Hutchison, V. Scardaci, A. C. Ferrari and J. N. Coleman, *Nature Nanotechnol.* 2008, **3**, 563-568.

9. H. Yang, F. Withers, E. Gebremedhn, E. Lewis, L. Britnell, A. Felten, V. Palermo, S. Haigh, D. Beljonne and C. Casiraghi, *2D Materials* 2008, **1**, 011012.